ACKNOWLEDGMENT

We are grateful to Professor Kazunari Akiyoshi for his generous cooperation in experiments. This research was supported in part by a Grant-in-Aid for Scientific Research from the Ministry of Education, Culture, Sports, Science and Technology, Japan, and Health and Labour Sciences Research Grants.

Supporting Information Available: Detailed materials and methods. This material is available free of charge via the Internet at http://pubs.acs.org.

LITERATURE CITED

(1) Oberlin, E., Amara, A., Bachelerie, F., Bessia, C., Virelizier, J. L., Arenzana-Seisdedos, F., Schwartz, O., Heard, J. M., Clark-Lewis, I., Legler, D. F., Loetscher, M., Baggiolini, M., and Moser, B. (1996) The CXC chemokine SDF-1 is the ligand for LESTR/fusin and prevents infection by T-cell-line-adapted HIV-1. *Nature 382*, 833–835.

(2) Bleul, C. C., Farzan, M., Choe, H., Parolin, C., Clark-Lewis, I., Sodroski, J., and Springer, T. A. (1996) The lymphocyte chemoattractant SDF-1 is a ligand for LESTR/fusin and blocks HIV-1 entry. *Nature 382*, 829–833.

(3) Baird, A. M., Gerstein, R. M., and Berg, L. J. (1999) The role of cytokine receptor signaling in lymphocyte development. *Curr. Opin. Immunol. 11*, 157–166.

(4) Koshiba, T., Hosotani, R., Miyamoto, Y., Ida, J., Tsuji, S., Nakajima, S., Kawaguchi, M., Kobayashi, H., Doi, R., Hori, T., Fujii, N., and Imamura, M. (2000) Expression of stromal cell-derived factor 1 and CXCR4 ligand receptor system in pancreatic cancer: a possible role for tumor progression. *Clin. Cancer Res. 6*, 3530–3535.

(5) Nanki, T., Hayashida, K., El-Gabalawy, H. S., Suson, S., Shi, K., Girschick, H. J., Yavuz, S., and Lipsky, P. E. (2000) Stromal cell-derived factor-1-CXC chemokine receptor 4 interactions play a central role in $CD4^+$ T cell accumulation in rheumatoid arthritis synovium. *J. Immunol. 165*, 6590–6598.

(6) Feng, Y., Broder, C. C., Kennedy, P. E., and Berger, E. A. (1996) HIV-1 entry cofactor: functional cDNA cloning of a seven-transmembrane, G protein-coupled receptor. *Science 272*, 872–7.

(7) Tamamura, H., Xu, Y., Hattori, T., Zhang, X., Arakaki, R., Kanbara, K., Omagari, A., Otaka, A., Ibuka, T., Yamamoto, N., Nakashima, H., and Fujii, N. (1998) A low-molecular-weight inhibitor against the chemokine receptor CXCR4: a strong anti-HIV peptide T140. *Biochem. Biophys. Res. Commun. 25*, 877–882.

(8) Fujii, N., Oishi, S., Hiramatsu, K., Araki, T., Ueda, S., Tamamura, H., Otaka, A., Kusano, S., Terakubo, S., Nakanishi, H., Broach, J. A., Trent, J. O., Wang, Z., and Peiper, S. C. (2003) Molecular-size reduction of a potent CXCR4-chemokine antagonist using orthogonal combination of conformation- and sequence-based libraries. *Angew. Chem., Int. Ed. 42*, 3251–3.

(9) Ichiyama, K., Yokoyama-Kumakura, S., Tanaka, Y., Tanaka, R., Hirose, K., Bannai, K., Edamatsu, T., Yanaka, M., Niitani, Y., Miyano-Kurosaki, N., Takaku, H., Koyanagi, Y., and Yamamoto, N. (2003) A duodenally absorbable CXC chemokine receptor 4 antagonist, KRH-1636, exhibits a potent and selective anti-HIV-1 activity. *Proc. Natl. Acad. Sci. U.S.A. 100*, 4185–4190.

(10) Donzella, G. A., Schols, D., Lin, S. W., Esté, J. A., Nagashima, K. A., Allaway, G. P., Sakmar, T. P., Henson, G., De Clercq, E., and Moore, J. P. (1998) AMD3100, a small molecule inhibitor of HIV-1 entry via the CXCR4 co-receptor. *Nat. Med. 4*, 72–77.

(11) Grynkiewicz, G., Poenie, M., and Tsien, R. Y. (1985) A new generation of Ca^{2+} indicators with greatly improved fluorescence properties. *J. Biol. Chem. 260*, 3440–3450.

(12) Kiyose, K., Kojima, H., Urano, Y., and Nagano, T. (2006) Development of a ratiometric fluorescent zinc ion probe in near-infrared region, based on tricarbocyanine chromophore. *J. Am. Chem. Soc. 128*, 6548–6549.

(13) Takakusa, H., Kikuchi, K., Urano, Y., Sakamoto, S., Yamaguchi, K., and Nagano, T. (2002) Design and synthesis of an enzyme-cleavable sensor molecule for phosphodiesterase activity based on fluorescence resonance energy transfer. *J. Am. Chem. Soc. 124*, 1653–1657.

(14) Kojima, H., Urano, Y., Kikuchi, K., Higuchi, T., Hirata, Y., and Nagano, T. (1999) Fluorescent indicators for imaging nitric oxide production. *Angew. Chem., Int. Ed. 38*, 3209–3212.

(15) Ojida, A., Mito-oka, Y., Sada, K., and Hamachi, I. (2004) Molecular recognition and fluorescence sensing of monophosphorylated peptides in aqueous solution by bis(zinc(II)-dipicolylamine)-based artificial receptors. *J. Am. Chem. Soc. 126*, 2454–2463.

(16) Tamamura, H., Omagari, A., Oishi, S., Kanamoto, T., Yamamoto, N., Peiper, S. C., Nakashima, H., Otaka, A., and Fujii, N. (2000) Pharmacophore identification of a specific CXCR4 inhibitor, T140, leads to development of effective anti-HIV agents with very high selectivity indexes. *Bioorg. Med. Chem. Lett. 10*, 2633–2637.

(17) Tamamura, H., Hiramatsu, K., Mizumoto, M., Ueda, S., Kusano, S., Terakubo, S., Akamatsu, M., Yamamoto, N., Trent, J. O., Wang, Z., Peiper, S. C., Nakashima, H., Otaka, A., and Fujii, N. (2003) Enhancement of the T140-based pharmacophores leads to the development of more potent and bio-stable CXCR4 antagonists. *Org. Biomol. Chem. 1*, 3663–3669.

(18) Hanaoka, H., Mukai, T., Tamamura, H., Mori, T., Ishinoa, S., Ogawa, K., Iida, Y., Doi, R., Fujii, N., and Saji, H. (2006) Development of a 111In-labeled peptide derivative targeting a chemokine receptor, CXCR4, for imaging tumors. *Nucl. Med. Biol. 33*, 489–494.

(19) Oishi, S., Masuda, R., Evans, B., Ueda, S., Goto, Y., Ohno, H., Hirasawa, A., Tsujimoto, G., Wang, Z., Peiper, S. C., Naito, T., Kodama, E., Matsuoka, M., and Fujii, N. (2008) Synthesis and application of fluorescein- and biotin-labeled molecular probes for the chemokine receptor CXCR4. *ChemBioChem 9*, 1154–1158.

(20) Futahashi, Y., Komano, J., Urano, E., Aoki, T., Hamatake, M., Yoshida, T., Koyanagi, Y., Matsuda, Z., and Yamamoto, N. (2007) Separate elements are required for ligand-dependent and -independent internalization of metastatic potentiator CXCR4. *Cancer Sci. 98*, 373–379.

(21) Tamamura, H., Ojida, A., Ogawa, T., Tsutsumi, H., Masuno, H., Nakashima, H., Yamamoto, N., Hamachi, I., and Fujii, N. (2006) Identification of a new class of low molecular weight antagonists against the chemokine receptor CXCR4 having the dipicolylamine-zinc(II) complex structure. *J. Med. Chem. 49*, 3412–3415.

(22) Trent, J. O., Wang, Z., Murray, J. L., Shao, W., Tamamura, H., Fujii, N., and Peiper, S. C. (2003) Lipid bilayer simulations of CXCR4 with inverse agonists and weak partial agonists. *J. Biol. Chem. 278*, 47136–47144.

(23) Valente, S. T., Chanel, C., Dumonceaux, J., Olivier, R., Marullo, S., Briand, P., and Hazan, U. (2001) CXCR4 is down-regulated in cells infected with the CD4-independent X4 human immunodeficiency virus type 1 isolate m7NDK. *J. Virol. 75*, 439–447.

(24) Orsini, M. J., Parent, J. L., Mundell, S. J., Marchese, A., and Benovic, J. L. (1999) Trafficking of the HIV coreceptor CXCR4. Role of arrestins and identification of residues in the C-terminal tail that mediate receptor internalization. *J. Biol. Chem. 274*, 31076–31086.

BC800216P

Structure-activity relationship study of CXCR4 antagonists bearing the cyclic pentapeptide scaffold: identification of the new pharmacophore†

Tomohiro Tanaka,[a] Hiroshi Tsutsumi,*[a] Wataru Nomura,[a] Yasuaki Tanabe,[a] Nami Ohashi,[a] Ai Esaka,[b] Chihiro Ochiai,[a] Jun Sato,[a] Kyoko Itotani,[a] Tsutomu Murakami,[c] Kenji Ohba,[c] Naoki Yamamoto,[c] Nobutaka Fujii[b] and Hirokazu Tamamura*[a]

Received 14th July 2008, Accepted 28th August 2008
First published as an Advance Article on the web 17th October 2008
DOI: 10.1039/b812029c

A highly potent CXCR4 antagonist **2** [cyclo (-D-Tyr[1]-Arg[2]-Arg[3]-Nal[4]-Gly[5]-)] has previously been identified by screening cyclic pentapeptide libraries that were designed based on pharmacophore residues of a 14-residue peptidic CXCR4 antagonist **1**. In the present study, D-Tyr and Arg in peptide **2** were replaced by a bicyclic aromatic amino acid and a cationic amino acid, respectively, and their binding activity for CXCR4 was evaluated for identification of the novel pharmacophore.

Introduction

The chemokine receptor CXCR4 is a membrane protein, which belongs to the G-protein coupled receptor family.[1,2] Interaction of CXCR4 with its endogenous ligand stromal-cell derived factor-1α (SDF-1α)/CXCL12 induces various physiological functions: chemotaxis,[3] angiogenesis,[4,5] neurogenesis,[6,7] *etc.* in embryonic stage. On the other hand, CXCR4 is also relevant to multiple diseases: AIDS,[8,9] cancer metastasis,[10] progress of leukemia,[11] rheumatoid arthritis,[12] *etc.* in adulthood. Actually, CXCR4 has been reported to be a potential drug target against these diseases. Thus, CXCR4 antagonists are useful for development of potent therapeutic agents against these diseases.[13-15] To date, various CXCR4 antagonists such as AMD3100[16,17] and KRH-1636[18] have been reported.

A β-sheet-like 14-residue peptide **1** was previously identified by structure optimization of an 18-residue cyclic peptide polyphemusin isolated from horseshoe crabs (Fig. 1).[19,20] In the downsizing of **1**, a cyclic pentapeptide **2** was developed by screening libraries based on four pharmacophore residues [Arg, Arg, 3-(2-naphthyl)alanine (Nal), D-Tyr] found by alanine scanning of **1**.[21]

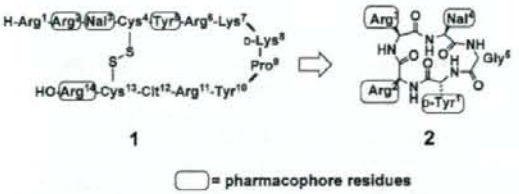

Fig. 1 Development of a cyclic pentapeptide **2** based the pharmacophore of a CXCR4 antagonistic peptide **1**. Cit = L-citrulline, Nal = L-3-(2-naphthyl)alanine.

We have studied structure-activity-relationships of **2** by various modifications.[22,23] In this paper, design of cyclic pentapeptide library based on the previous structure-activity relationship data led to development of novel analogues of **2** to explore new pharmacophore moieties.

Biological results and discussion

Substitution of a large aromatic amino acid for D-Tyr[1] of 2

Our previous data of alanine-scanning of **2** suggested that D-Tyr[1] or Arg[2] was not optimalized.[24] Thus, we attempted to replace these functional groups. According to other previous reports, potent CXCR4 antagonists absolutely contain aromatic and cationic groups.[25] It suggests that these functional groups are involved in binding to CXCR4 mediated by hydrophobic and electrostatic interaction. To evaluate significance of the hydrophobic interaction by aromatic rings, D-Tyr[1] of **2** was replaced by an L/D-bicyclic aromatic amino acid. In addition, four epimers were synthesized to evaluate effects of configuration of amino acids of the 1- and 2- positions (Fig. 2). Compounds **3c** and **3d** with replacement of D-Tyr[1] by D-3-(1-naphthyl)alanine (D-Nal(1)) showed high CXCR4 binding activity (IC_{50} = 0.043 and 0.078 μM, respectively, Table 1), although the potencies were approximately one-third or fifth of that of the parent compound **2** (IC_{50} = 0.015 μM, Table 1). Similarly, compounds **5c** and **5d**, replaced by D-Trp at the 1-position, showed 5–10 fold lower CXCR4 binding activity (IC_{50} = 0.15 and 0.070 μM, respectively, Table 1) than the parent compound **2**. On the other hand, compounds **4c** and **4d** did not show strong CXCR4 binding activity. These data indicates that the spatial position of aromatic ring is essential for the expression of CXCR4 binding activity. In addition, a series of **a** or **b** except for **5a** did not show strong CXCR4 binding activity (all IC_{50} values > 0.3 μM, Table 1). These data indicate that the chirality of L/D-Arg[2] was not important for the expression of CXCR4 binding activity, whereas the chirality of Nal(1)[1] and Trp[1] is influential. The

[a]*Institute of Biomaterials and Bioengineering, Tokyo Medical and Dental University, Chiyoda-ku, Tokyo, 101-0062, Japan. E-mail: tsutsumi.mr@tmd.ac.jp, tamamura.mr@tmd.ac.jp; Fax: 813 5280 8039; Tel: 813 5280 8036*
[b]*Graduate School of Pharmaceutical Sciences, Kyoto University, Sakyo-ku, Kyoto, 606-8501, Japan*
[c]*AIDS Research Center, National Institute of Infectious Diseases, Shinjuku-ku, Tokyo, 162-8640, Japan*

† Electronic supplementary information (ESI) available: Characterization data (MS) of novel synthetic compounds. See DOI: 10.1039/b812029c

This journal is © The Royal Society of Chemistry 2008

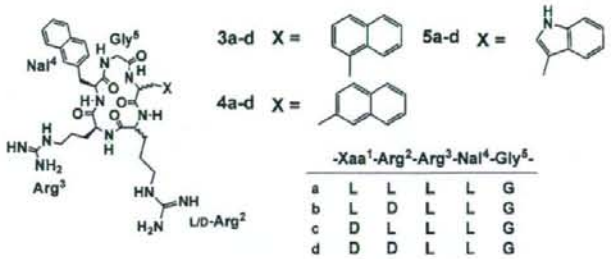

Fig. 2 Structures of compounds having substitution of an L/D- bicyclic aromatic amino acid for Tyr[1].

Table 1 Inhibitory activities of the synthetic compounds against binding of [^{125}I]-SDF-1α to CXCR4

Compound no.	IC_{50}/μM[a]	Compound no.	IC_{50}/μM[a]
2	0.015	**3c**	0.043
3a	0.3–2.0	**4c**	> 2.0
4a	0.3–2.0	**5c**	0.15
5a	0.22	**3d**	0.078
3b	0.3–2.0	**4d**	0.3–2.0
4b	0.3–2.0	**5d**	0.070
5b	> 2.0		

[a] IC_{50} values are the concentrations for 50% inhibition of the [^{125}I]-SDF-1 binding to Jurkat cells. All data are the mean values for at least three experiments.

Table 2 Inhibitory activities of the synthetic compounds against binding of [^{125}I]-SDF-1α to CXCR4

Compound no.	IC_{50}/μM[a]	Compound no.	IC_{50}/μM[a]
2	0.015	**6c**	0.3–2.0
6a	> 2.0	**7c**	0.3–2.0
7a	0.3–2.0	**8c**	> 2.0
8a	> 2.0	**6d**	> 2.0
6b	> 2.0	**7d**	0.3–2.0
7b	0.045	**8d**	0.3–2.0
8b	> 2.0		

[a] IC_{50} values are the concentrations for 50% inhibition of the [^{125}I]-SDF-1 binding to Jurkat cells. All data are the mean values for at least three experiments.

dependence of CXCR4 binding activity on the chirality at the 1-position might be caused by a conformational change of the peptide backbone.

Shuffling cationic and aromatic amino acids at the 1- and 2-positions of cyclic pentapeptides

An analogue of **2**, having substitution of Arg[1] and D-4F-phenylalanine[2] for D-Tyr[1] and Arg[2], respectively, was recently found as a strong CXCR4 antagonist.[22] To evaluate effects of the sequential difference of cationic and aromatic groups at the 1- and 2-positions on CXCR4 binding activity, Arg and a large aromatic amino acid (Nal(1), Nal or Trp) were shuffled in the pentapeptide, and four epimers were synthesized in a similar manner (Fig. 3). Synthetic compounds except for **7b** did not show CXCR4 binding activity up to 0.3 μM (Table 2). In particular, a series of **6** and **8** did not show CXCR4 binding activity despite of difference of the chilality of amino acids at the 1- and 2-positions (**6c**, **8d** > 0.3 μM, **6a**, **6b**, **6d**, **8a**, **8b**, **8c** > 2.0 μM). On the other hand, a series of **7**, which introduced L/D-Nal at the 2-position, did not show a serious reduction of CXCR4 binding activity. These data indicated that Nal(1) or Trp might not be appropriate as the amino acid introduced at the 2-position, possibly due to spatial configuration of aromatic rings. **7b** showed the highest CXCR4 binding activity among compounds in this library. Interestingly, **7b** has the opposite chirality and order of the aromatic residue at the 1- and 2-positions compared to the parent compound **2**.

Evaluation of anti-HIV activity and cytotoxicity

Anti-HIV activity and cytotoxicity of compounds **5c**, **5d** and **7b** that showed moderate CXCR4 binding activity and have a characteristic sequence and conformation were evaluated. Since CXCR4 is a coreceptor for an X4-HIV-1 entry, CXCR4 antagonists have anti-HIV activity.[8,9] Anti-HIV activities of compounds **5d** and **7b** (EC_{50} = 0.19 and 0.26 μM, respectively, Table 3) were nearly equal

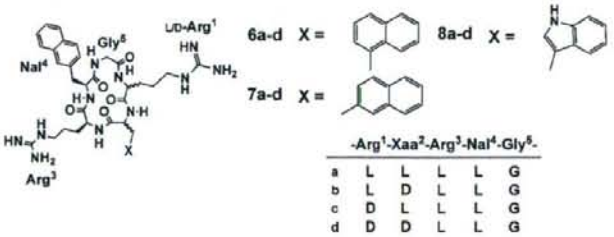

Fig. 3 Structures of compounds having L/D-Arg[1] and an L/D-bicyclic aromatic amino acid.[2]

Table 3 Anti-HIV activity and cytotoxicity of the synthetic compounds

Compound no.	EC_{50}/μM[a]	CC_{50}/μM[b]
AZT	0.077	> 10
1	0.044	> 10
2	0.15	> 10
5c	0.70	> 10
5d	0.19	> 10
7b	0.26	> 10

[a] EC_{50} values are based on the inhibition of HIV-induced cytopathogenicity in MT-4 cells. [b] CC_{50} values are based on the reduction of the viability of MT-4 cells. All data are the mean values for at least three experiments.

to that of **2** (EC_{50} = 0.15 μM, Table 3). Interestingly, CXCR4 binding activity of **5d** (IC_{50} = 0.070 μM, Table 1) was lower than that of **7b** (IC_{50} = 0.045 μM), whereas anti-HIV activity of **5d** (EC_{50} = 0.19 μM, Table 3) was slightly higher than that of **7b** (EC_{50} = 0.26 μM). In addition, all tested compounds did not show significant cytotoxicity (CC_{50} > 10 μM, Table 3).

Conclusion

Our first approach screening cyclic pentapeptides, which have substitution of a bicyclic aromatic amino acid at the 1-position, disclosed that D-3-(1-naphthyl)alanine and D-Trp at the 1-position might be alternative pharmacophore moieties, and that introduction of D-amino acid at the 1-position was required to form an optimal cyclic pentapeptide backbone. In addition, compound **5d** showed high anti-HIV activity, comparable to that of compound **2**.

A cyclic pentapeptide library based on shuffling cationic and aromatic amino acids at the 1- and 2-positions of compound **2** was designed. As a result, the order of a cationic amino acid and an aromatic amino acid is significant to maintain strong CXCR4 binding activity of analogues of **2**. Compound **7b**, however, showed the highest CXCR4 binding activity among the present synthetic cyclic pentapeptides. **7b** was proven to be a new type lead, because of the difference of the order of cationic and aromatic residues, and also showed high anti-HIV activity. Finding of compound **7b** indicated that Arg^1 and D-Nal^2 may be novel pharmacophore moieties in the combination with Nal^4 and Arg^5. To date, pharmacophore functional groups have been identified to be two guanidino, naphthyl and phenol groups derived from two Arg, Nal and D-Tyr in the cyclic pentapeptide scaffolds. In this study, only guanidino and naphthyl groups have been proven to be indispensable for CXCR4 binding activity. The present data will provide useful approaches for simple designs of new low molecular weight CXCR4 antagonists. These results might also give valuable insights for understanding the ligand-receptor interactions.

Experimental

Chemistry

Cyclic peptides were synthesized by Fmoc-based solid-phase synthesis on 2-Chlorotrityl resin followed by cleavage from the resin, cyclization with the diphenylphosphoryl azide and deprotection, as reported previously.[23]

Cell culture

Human T-cell lines, Jurkat cells and MT-4 cells were grown in RPMI 1640 medium containing 10% heat-inactivated fetal calf serum.

Virus

An X4 HIV-1 infectious molecular clone pNL4-3 was obtained from the AIDS Research and Reference Reagent Program.[26] The virus NL4-3 was obtained from the culture supernatant of 293T cells transfected with the pNL4-3. Aliquots of the viral stocks were stored at −80 °C until use. The titer of virus stocks was determined by endpoint titration of 5-fold limiting dilutions in MT-4 cells.

CXCR4 receptor binding assay

Jurkat cells were harvested and centrifugated at 1000 rpm for 5 min. Cells were then resuspended in RPMI buffer (20 mM HEPES, 0.5% bovine serum albumin) and placed in silicone-coated tubes (5.0×10^5 cells/120 μL). Cold SDF-1 (final concentration 1 μM, 15 μL/well) and various concentrations of test compounds (10% DMSO, 15 μL/well) were added to the above tubes followed by addition of [^{125}I]-SDF-1 (Perkin-Elmer Life Sciences, 0.05 nM, 15 μL/well). After 1 h's incubation on ice, oil (dibutyl phthalate:olive oil = 4:1 (v/v), 500 μL/well) was added followed by centrifugation at 14,000 rpm for 2 min. After removal of aqueous and organic layers and cutting the bottoms from the tubes, the bottoms were placed in RIA-tubes and the CPM was counted by γ-counter. Inhibition percentage of FC131 analogs against the binding of [^{125}I]-SDF-1 was calculated by the following equation.[27]

Inhibition (%) = (Et–Ea)/(Et–Ec) × 100

Et: the quantity of radioactivity in the absence of a test compound

Ec: the quantity of radioactivity in the presence of cold SDF-1α as a test compound

Ea: the quantity of radioactivity in the presence of a test compound

Anti-HIV assay

Anti-HIV-1 activity was determined based on the protection against HIV-1-induced cytopathogenicity in MT-4 cells. Various concentrations of test compounds were added to HIV-1 infected MT-4 cells at multiplicity of infection (MOI) of 0.001 and placed in wells of a flat-bottomed microtiter tray (2.0×10^4 cells/well). After 5 days' incubation at 37 °C in a CO_2 incubator, the number of viable cells was determined using the 3-(4,5-dimethylthiazol-2-yl)-2,5-diphenyltetrazolium bromide (MTT) method.

Acknowledgements

This work was supported by Grant-in-Aid for Scientific Research from the Ministry of Education, Culture, Sports, Science, and Technology of Japan, and Health and Labour Sciences Research Grants from Japanese Ministry of Health, Labor, and Welfare.

References

1 M. Loetscher, T. Geiser, T. O'Reilly, R. Zwahlen, M. Baggiolini and B. Moser, *J. Biol. Chem*, 1994, **269**, 232–237.

This Journal is © The Royal Society of Chemistry 2008

2 B. J. Rollins, *Blood*, 1997, **90**, 909–928.
3 C. C. Bleul, R. C. Fuhlbrigge, J. M. Casanovas, A. Aiuti and T. A. Springer, *J. Exp. Med.*, 1996, **2**, 1101–1109.
4 K. Tachibana, S. Hirota, H. Iizasa, H. Yoshida, K. Kawabata, Y. Kataoka, Y. Kitamura, K. Matsushima, N. Yoshida, S. Nishikawa, T. Kishimoto and T. Nagasawa, *Nature*, 1998, **393**, 591–594.
5 T. Nagasawa, S. Hirota, K. Tachibana, N. Takakura, S. Nishikawa, Y. Kitamura, N. Yoshida, H. Kikutani and T. Kishimoto, *Nature*, 1996, **382**, 635–638.
6 Y. Zhu, Y. Yu, X. C. Zhang, T. Nagasawa, J. Y. Wu and Y. Rao, *Nat. Neurosci.*, 2002, **5**, 719–720.
7 R. K. Stumm, C. Zhou, T. Ara, F. Lazarini, M. Dubois-Dalcq, T. Nagasawa, V. Hollt and S. Schulz, *J. Neurosci.*, 2003, **23**, 5123–5130.
8 E. Oberlin, A. Amara, F. Bachelerie, C. Bessia, J. L. Virelizier, F. Arenzana-Seisdedos, O. Schwartz, J. M. Heard, I. Clark-Lewis, D. L. Legler, M. Loetscher, M. Baggiolini and B. Moser, *Nature*, 1996, **382**, 833–835.
9 Y. Feng, C. C. Broder, P. E. Kennedy and E. A. Berger, *Science*, 1996, **272**, 872–877.
10 A. Müller, B. Homey, H. Soto, N. Ge, D. Catron, M. E. Buchanan, T. Mcclanahan, E. Murphy, W. Yuan, S. M. Wagner, J. L. Barrera, A. Mohar, E. Vera'stegui and A. Zlotnik, *Nature*, 2001, **410**, 50–56.
11 J. A. Burger, M. Burger and T. J. Kipps, *Blood*, 1999, **94**, 3658–3667.
12 T. Nanki, K. Hayashida, H. S. El-Gabalawy, S. Suson, K. Shi, H. J. Girschick, S. Yavuz and P. E. Lipsky, *J Immunol*, 2000, **165**, 6590–6598.
13 T. Murakami, T. Nakajima, Y. Koyanagi, K. Tachibana, N. Fujii, H. Tamamura, N. Toshida, M. Waki, A. Matsumoto, O. Yoshie, T. Kishimoto, N. Yamamoto and T. Nagasawa, *J. Exp. Med.*, 1997, **186**, 1389–1393.
14 H. Tamamura, A. Hori, N. Kanzaki, K. Hiramatsu, M. Mizumoto, H. Nakashima, N. Yamamoto, A. Otaka and N. Fujii, *FEBS Lett.*, 2003, **550**, 79–83.
15 H. Tamamura, M. Fujisawa, K. Hiramatsu, M. Mizumoto, H. Nakashima, N. Yamamoto, A. Otaka and N. Fujii, *FEBS Lett.*, 2004, **569**, 99–104.
16 D. Schols, S. Struyf, J. Van Damme, J. A. Este, G. Henson and E. DeClarcq, *J. Exp. Med.*, 1997, **186**, 1383–1388.
17 G. A. Donzella, D. Schols, S. W. Lin, J. A. Este and K. A. Nagashima, *Nat. Med.*, 1998, **4**, 72–76.
18 K. Ichiya, S. Yokoyama-Kumakura, Y. Tanaka, R. Tanaka, K. Hirose, K. Bannai, T. Edamatsu, M. Yanaka, Y. Niitani, N. Miyano-Kurosaki, H. Takaku, Y. Koyanagi and N. Yamamoto, *Proc. Natl. Acad. Sci. USA*, 2003, **100**, 4185–4190.
19 Tamamura, Y. Xu, T. Hattori, X. Zhang, R. Arakaki, K. Kanbara, A. Omagari, A. Otaka, T. Ibuka, N. Yamamoto, H. Nakashima and N. Fujii, *Biochem. Biophys. Res. Commun.*, 1998, **253**, 877–882.
20 M. Masuda, H. Nakashima, T. Ueda, H. Naba, R. Ikoma, A. Otaka, Y. Terakawa, H. Tamamura, T. Ibuka, T. Murakami, Y. Koyanagi, M. Waki, A. Matsumoto, N. Yamamoto and N. Fujii, *Biochem. Biophys. Res. Commun.*, 1992, **189**, 845–850.
21 N. Fujii, S. Oishi, K. Hiramatsu, T. Araki, S. Ueda, H. Tamamura, A. Otaka, S. Kusano, S. Terakubo, H. Nakashima, J. A. Broach, J. O. Trent, Z. Wang and S. C. Peiper, *Angew. Chem. Int. Ed.*, 2003, **42**, 3251–3253.
22 H. Tamamura, T. Araki, S. Ueda, Z. Wang, S. Oishi, A. Esaka, J. O. Trent, H. Nakashima, N. Yamamoto, S. C. Peiper, A. Otaka and N. Fujii, *J. Med. Chem.*, 2005, **48**, 3280–3289.
23 H. Tamamura, A. Esaka, T. Ogawa, T. Araki, S. Ueda, Z. Wang, J. O. Trent, H. Tsutsumi, H. Masuno, H. Nakashima, N. Yamamoto, S. C. Peiper, A. Otaka and N. Fujii, *Org. Biomol. Chem.*, 2005, **3**, 4392–4394.
24 S. Ueda, S. Oishi, Z. Wang, T. Araki, H. Tamamura, J. Cluzeau, H. Ohno, S. Kusano, H. Nakashima, J. O. Trent, S. C. Peiper and N. Fujii, *J. Med. Chem.*, 2007, **50**, 192–198.
25 W. Zhan, Z. Liang, A. Zhu, S. Kurtkaya, H. Shim, J. P. Snyder and D. C. Liotta, *J.Med. Chem.*, 2007, **50**, 5655–5664.
26 A. Adachi, H. E. Gendelman, S. Koenig, T. Folks, R. Willey, A. Rabson and M. A. Martin, *J Virol.*, 1986, **59**, 284–291.
27 H. Tamamura, K. Hiramatsu, S. Kusano, S. Terakubo, N. Yamamoto, J. O. Trent, Z. Wang, S. C. Peiper, H. Nakashima, A. Otaka and N. Fujii, *Org. Biomol. Chem.*, 2003, **1**, 3656–3662.

JOURNAL OF VIROLOGY, May 2007, p. 4445–4456
0022-538X/07/$08.00+0 doi:10.1128/JVI.00026-07
Copyright © 2007, American Society for Microbiology. All Rights Reserved.
Vol. 81, No. 9

Simian Immunodeficiency Virus (SIV) Infection Influences the Level and Function of Regulatory T Cells in SIV-Infected Rhesus Macaques but Not SIV-Infected Sooty Mangabeys▽

L. E. Pereira,[1] F. Villinger,[1] N. Onlamoon,[1,2] P. Bryan,[1] A. Cardona,[1] K. Pattanapanysat,[2,3] K. Mori,[4]† S. Hagen,[5] L. Picker,[5] and A. A. Ansari[1]*

Department of Pathology and Lab Medicine, Emory University School of Medicine, Atlanta, Georgia[1]; Department of Immunology, Siriraj Hospital, Mahidol University, Bangkok, Thailand[2]; Thailand Research Fund[3]; Tsukuba Primate Center, NIH, Japan[4]; and Oregon Health and Science University and Oregon National Primate Research Center, Portland, Oregon[5]

Received 4 January 2007/Accepted 12 February 2007

Differences in clinical outcome of simian immunodeficiency virus (SIV) infection in disease-resistant African sooty mangabeys (SM) and disease-susceptible Asian rhesus macaques (RM) prompted us to examine the role of regulatory T cells (Tregs) in these two animal models. Results from a cross-sectional study revealed maintenance of the frequency and absolute number of peripheral Tregs in chronically SIV-infected SM while a significant loss occurred in chronically SIV-infected RM compared to uninfected animals. A longitudinal study of experimentally SIV-infected animals revealed a transient increase in the frequency of Tregs from baseline values following acute infection in RM, but no change in the frequency of Tregs occurred in SM during this period. Further examination revealed a strong correlation between plasma viral load (VL) and the level of Tregs in SIV-infected RM but not SM. A correlation was also noted in SIV-infected RM that control VL spontaneously or in response to antiretroviral chemotherapy. In addition, immunofluorescent cell count assays showed that while Treg-depleted peripheral blood mononuclear cells from RM led to a significant enhancement of $CD4^+$ and $CD8^+$ T-cell responses to select pools of SIV peptides, there was no detectable T-cell response to the same pool of SIV peptides in Treg-depleted cells from SIV-infected SM. Our data collectively suggest that while Tregs do appear to play a role in the control of viremia and the magnitude of the SIV-specific immune response in RM, their role in disease resistance in SM remains unclear.

African primate sooty mangabeys (SM) (*Cercocebus atys*) are a natural host of simian immunodeficiency virus (SIV) but remain asymptomatic throughout the course of infection and do not develop any detectable immunodeficiency or disease. Despite high viremia, naturally or experimentally SIV-infected SM maintain reasonable CD4 T-cell counts and an absence of chronic activation of T cells (10, 33, 39). This symptom-free characteristic of SM is in marked contrast to the CD4 T-cell depletion and disease progression that occur in SIV-infected Asian rhesus macaques (RM) (21, 38). In the latter species, the initial CD8 T-cell-mediated antiviral response generated during the acute phase, although beneficial, proves to be inadequate for viral control and clearance, resulting in chronic viremia and a state of chronic immune activation (24, 34, 38). The increased levels of activation-induced cell death and to various levels bystander apoptosis exhibited by SIV-infected RM are markedly attenuated or absent in SIV-infected SM (38, 39). Since viral loads (VL) in SIV-infected SM reach levels that lead to AIDS in the vast majority of similarly infected RM, the development of disease in the latter species is believed to depend on the quality and/or quantity of the immune response to viral infection rather than VL alone.

While both RM and SM develop readily detectable anti-SIV-specific antibodies following infection, the magnitude of $CD4^+$ and $CD8^+$ SIV-specific cellular immune responses in SIV-infected SM is typically diminished and difficult to detect in comparison to the elevated T-cell SIV-specific immune response in SIV-infected RM (10, 38). It was reasoned that one explanation for the limited virus-specific cellular immune response exhibited by SIV-infected SM could be that this response is secondary to the effect of more-potent and/or a higher level of natural regulatory T cells (Tregs), a cell lineage that has recently been revisited for its role in SIV/human immunodeficiency virus (HIV) pathogenesis. Tregs typically constitute a small percentage of circulating $CD4^+$ T cells (2 to 5% in adult humans) (4, 20, 25, 35). Markers commonly associated with the identification of Tregs include high cell surface levels of the interleukin-2 receptor alpha (IL-2Rα) CD25 and the transcription factor FoxP3 (4, 20, 35, 41, 48). Additional markers include cytotoxic-T-lymphocyte-associated antigen 4, GITR, low levels of the more recently identified Treg marker IL-7 receptor CD127 (26, 27, 37, 43), and, more recently, unique microRNA profiles (9). $CD4^+$ $CD25^{hi}$ Tregs inhibit proliferation of T cells primarily through contact-dependent mechanisms, although cytokine (IL-10 and transforming growth factor β [TGF-β])-mediated inhibition has also been suggested previously (2, 5, 20, 25, 28, 31, 32).

Conflicting data regarding the role of Tregs in lentiviral infection are not uncommon, with some studies suggesting that

* Corresponding author. Mailing address: Department of Pathology and Lab Medicine, Emory University School of Medicine, 101 Woodruff Circle, Rm. 2309, Atlanta, GA 30329. Phone: (404) 712-2834. Fax: (404) 712-1771. E-mail: pathaaa@emory.edu.

† Present address: AIDS Research Center, National Institute of Infectious Disease, Tokyo, Japan.

▽ Published ahead of print on 21 February 2007.

the level of Tregs is unaffected by infection and others showing either an expansion or a decline in Tregs in SIV/HIV-infected hosts (1, 3, 12, 22, 29, 30, 45, 47). This apparent disparity is in part due to differences in the chosen marker(s) for Treg identification, the lack of optimized techniques utilized for Treg quantification (cellular gene expression versus flow cytometry) and data analysis (frequency versus absolute numbers [ABS]), and the stage of infection at the time of sampling. To gain a better understanding of Treg dynamics in SIV pathogenesis, we performed a comprehensive study involving the phenotypic analysis of Tregs from peripheral blood mononuclear cells (PBMCs) from uninfected and SIV-infected SM and RM during the acute, early chronic, and late chronic stages of infection. The effect of antiretroviral therapy (ART) on Treg levels in SIVmac-infected RM was also determined. In addition, a characterization of Treg function in SIV-infected RM and SM was performed. The basic aim of this study is twofold: first, to determine the relationship, if any, between SIV infection and the level and/or function of Tregs in RM and SM, and second, to determine if this cell lineage plays a role in the SIV-specific adaptive immune response and/or generalized immune activation that is muted in SIV-infected SM but readily exhibited by SIV-infected RM. Our results suggest a decline in the number of Tregs in SIV-infected RM and a correlation between Tregs and levels of VL and controlled immune activation in this species. However, the frequency and ABS of Tregs alone cannot account for either VL or disease resistance in the SIV-infected SM.

MATERIALS AND METHODS

Animals and infections. The healthy uninfected and the SIV-infected RM and SM were housed at Yerkes Regional Primate Research Center (YRPRC) of Emory University or at the Oregon National Primate Research Center (ONPRC) at the University of Oregon. Their housing, care, diet, and maintenance conformed to the guidelines of the Committee on the Care and Use of Laboratory Animals of the Institute of Laboratory Animal Resources, National Research Council, and the Health and Human Services guidelines *Guide for the Care and Use of Laboratory Animals* (28a). The sources of the samples from the SIV-infected animals were as follows.

(i) SM. The SIV-noninfected SM and SM that were naturally infected were of comparable ages and were part of breeding colonies maintained at the YRPRC field station. A group of SIV-negative SM were experimentally infected with SIV (a viral stock of an isolate from a mangabey, FUo, that readily infects and replicates in SM monkeys; courtesy of S. Staprans, Emory University) and were housed in individual cages at the main station of the YRPRC. These monkeys served as a source for the longitudinal SM study.

(ii) RM. RM involved in the longitudinal study consisted of two groups of animals: one group was infected intravenously with 200 50% tissue culture infective doses of SIVmac239, and the other was infected with 10,000 50% tissue culture infective doses. A subset of the latter group of SIVmac239-infected RM were treated with PMPA (9-(2-phosphonomethoxypropyl)adenine) (20 mg/kg of body weight subcutaneously daily for 28 days after reaching the VL set point) and were utilized to study the effects of antiviral therapy on Tregs. All uninfected and SIV-infected RM used in the study were of comparable ages.

Specimen collection. PBMCs were isolated by standard Ficoll-Hypaque gradient centrifugation from whole blood. White blood cell, platelet, and total lymphocyte counts were determined using standard methods and used to calculate absolute values. Lymph nodes and various tissues were obtained at necropsy from five uninfected RM and four SIVmac239-infected RM that were sacrificed due to end-stage AIDS. Single-cell suspensions of lymph node cells were obtained by teasing the cells out of the respective nodes. Mucosal intraepithelial and lamina propria lymphocytes were obtained after serial incubation in EDTA, digestion with collagenase (Worthington type IV), and purification/enrichment on discontinuous 30/60% Percoll gradients.

Flow cytometry analysis. Multiple monoclonal antibodies (MAb) with specificity for human CD4, CD25, FoxP3, GITR, and CD127 were first screened in multiple combinations with a variety of fixing conditions to identify those that provided optimal data (similar to human Tregs) for the identification of RM and SM Tregs. From the list of clones screened, the following antibody clones were selected for the immunophenotyping studies of Tregs reported herein: CD4-peridinin chlorophyll protein (clone L200), CD127-phycoerythrin (PE), CD95-fluorescein isothiocyanate (FITC) (clone DX-2) (all purchased from BD Pharmingen, San Diego, CA), CD25-PE (clone 4E3; Miltenyi Biotec, Auburn, CA), and FoxP3-allophycocyanin (clone PCH101 or 236A/E7; E-Bioscience, San Diego, CA). Cells were first incubated with 1 μg/ml of anti-FcR antibody (clone 2.4G2; courtesy of R. Mittler, Emory University) for 15 min at 4°C, washed, and then surface stained for 15 min at 4°C with predetermined optimal concentrations of CD4-peridinin chlorophyll protein, CD95-FITC, and CD25-PE or CD127-PE. Fixation and intracellular staining to detect FoxP3 were performed according to an E-Biosciences protocol. Appropriate MAb isotype controls were included. The study of cell activation markers included the use of MAb against CD25 (Miltenyi Biotec), CD69 (clone FN50; BD Pharmingen), and HLA-DR (clone L243; BD Pharmingen). Flow cytometric acquisition of at least 100,000 events from each sample was performed on a FACSCalibur flow cytometer. Samples were also analyzed on an LSR II system by use of the following panel: CD4-AmCyan (L200) and CD95-PECy7 (DX2), both from BD Biosciences; CD25-biotin (4E3; Miltenyi); streptavidin-ECD (Beckman-Coulter, Miami, FL); and FoxP3-PE (206D; BioLegend, San Diego, CA). Data acquisition and analysis were done using CellQuest (BD Biosciences) and FlowJo (TreeStar, Ashland, OR) software, respectively. Data reported herein represent results acquired utilizing the FACSCalibur system.

Cell isolation and in vitro suppression/MLR assays. $CD4^+$ T cells were isolated from PBMCs by negative selection using an RM CD4 T-cell enrichment kit (StemCell Technologies, Inc.). Enriched cells were stained with CD25-PE (5 μl/million cells) for 15 min at 4°C. $CD4^+$ $CD25^+$ Treg cells were purified using an anti-PE EasySep kit (StemCell Technologies, Inc.). Flow cytometry was performed on aliquots to confirm the phenotype of the isolated responder cells ($CD4^+$ $CD25^-$) and that of Tregs ($CD4^+$ $CD25^+$). In vitro mixed lymphocyte reaction (MLR) assays were performed to assess Treg function. Briefly, highly enriched populations of responder $CD4^+$ T cells depleted of $CD25^+$ T cells were incubated in triplicate with a fixed number of a pool of allogeneic irradiated stimulator cells in a 96-well plate in the absence and presence of graded numbers of $CD4^+$ $CD25^{hi}$ cells (autologous to the responder cells). The cultures were incubated for 5 days at 37°C and 5% CO_2. Sixteen hours prior to harvest, cells were pulsed with 1 μCi/well ^{3}[H]thymidine. Cultures were harvested and the mean uptake of ^{3}[H]thymidine determined using standard scintillation counting. One unit of Treg function was defined as the number of Tregs that inhibited the *allo*-MLR by 1/3. In addition, an *allo*-MLR precursor frequency was determined, using highly enriched $CD4^+$ T cells with and without depletion of the $CD4^+$ $CD25^+$ T cells. Various numbers of these responder cells were cocultured with a fixed number of an irradiated mixed pool of stimulator cells, with each dilution cocultured in 24 replicate wells. The number of wells showing significant proliferation was defined as individual wells showing uptake of ^{3}[H]thymidine, which was 3 standard deviations (SD) above the mean value of the appropriate number of responder cells cultured alone. The *allo*-reactive precursor frequencies were estimated based on the "single hit" Poisson model as described by Strijbosch et al. (40), who kindly supplied us with software for the analyses performed herein.

Determination of SIV antigen-specific $CD4^+$ and $CD8^+$ responses. Aliquots of unfractionated or $CD4^+$/$CD25^+$-depleted PBMCs from each monkey were cultured for 2 h with eight individual pools of overlapping SIV Env peptides (25-mers overlapping by 13) or eight individual pools of overlapping Gag peptides (20-mers overlapping by 12) covering the entire SIV env and gag region (based on the SIVmac239 sequence), followed by the addition of brefeldin A and incubation overnight. Cells were then washed and surface stained for CD4 and CD8 (CD8-FITC; BD Pharmingen) and then fixed/permeabilized and stained for intracellular gamma interferon (IFN-γ) (allophycocyanin conjugated; BD Pharmingen). The frequency of IFN-γ-producing $CD4^+$ or $CD8^+$ cells was determined by standard flow cytometric analysis.

Determination of VL. Plasma VL were determined by the Virology Core of the Emory University CFAR by use of a competitive reverse transcriptase PCR assay.

Statistical analysis. Data are represented as means ± SD and were analyzed by using the two-tailed Student *t* test. A linear least-square regression model and the Mann-Whitney test (two tailed) were used to derive a correlation between VL and Tregs. A P value of <0.05 was considered to be statistically significant.

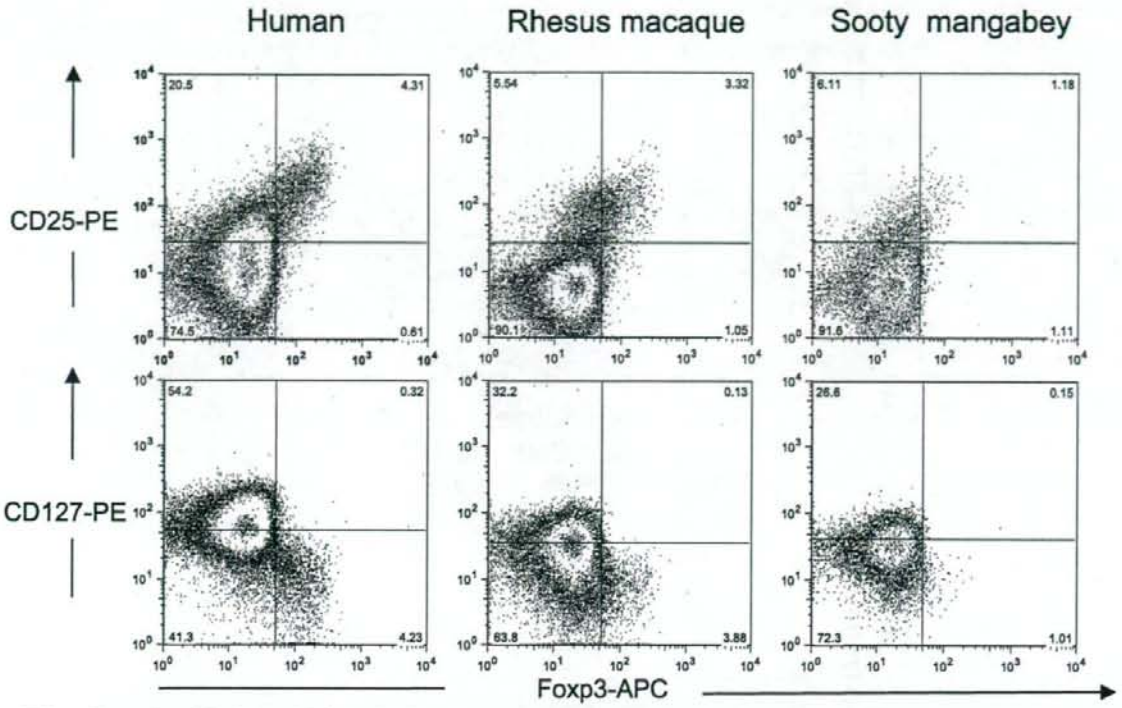

FIG. 1. Expression of FoxP3 on CD4$^+$ T cells from humans and the nonhuman primates RM and SM. PBMCs from uninfected human volunteers, RM, and SM were stained for cell surface expression of CD4 and CD25 or CD127. The stained cells were fixed and stained intracellularly with anti-FoxP3. Shown are representative profiles for each species. The number in each quadrant indicates the frequency of gated CD4$^+$ T cells that express the relevant marker. APC, allophycocyanin.

RESULTS

Expression of CD127^{lo} or CD25^{hi} in combination with FoxP3 enables Treg identification in both SM and RM. Recent studies have demonstrated that the cell surface expression of CD127^{lo} in combination with CD25$^+$ or in combination with FoxP3 can be used to accurately identify Treg subsets in human peripheral blood (26, 37). To determine if a similar method can be applied to nonhuman primates, PBMCs were isolated from uninfected SM (n = 12) and RM (n = 12), and the CD25^{hi} FoxP3$^+$ or CD127^{lo} FoxP3$^+$ population within the total CD4$^+$ T-cell population was measured. PBMCs from healthy adult human volunteers (n = 3) were also analyzed for comparison. As indicated by the representative flow cytometric profiles in Fig. 1, the frequency of CD4$^+$ CD25^{hi} FoxP3$^+$ cells was similar to that of the CD4$^+$ CD127^{lo} FoxP3$^+$ subset for each species. On average, the percentage of CD4$^+$ CD25^{hi} FoxP3$^+$ cells was lower in RM (3.0% ± 0.59%) than in humans (4.33% ± 0.15%), and SM expressed the lowest frequency of Tregs (1.9% ± 0.47%). This difference in cell frequency was reflected in the ABS of Tregs, with RM possessing about a twofold-greater level of Tregs than SM (Table 1). This apparent species-specific difference may be secondary to various levels of cross-reactivity with the FoxP3 MAb, although staining with two additional FoxP3-specific MAb clones generated similar results. There was no significant difference in mean density of FoxP3 expression in RM and SM (data not shown). Thus, it appears that the conventional Treg markers CD25^{hi} and FoxP3 can be utilized to identify Tregs in RM and even SM, in agreement with a recent study (42), and the data are also supported by the results obtained by functional assays, such as

TABLE 1. Frequencies and ABS of Tregs within the total CD4$^+$ T-cell population and the memory and naïve CD4$^+$ T-cell subsets in uninfected (SIV$^-$) and SIV-infected (SIV$^+$) RM and SM from a cross-sectional study[a]

CD4$^+$ population	Primate species and SIV infection status	Frequency of Tregs	ABS of Tregs/μl blood
Total	SIV$^-$ SM	1.9 ± 0.47	28 ± 13
	SIV$^+$ SM	1.66 ± 0.45	18 ± 7
	SIV$^-$ RM	3 ± 0.59	66 ± 16
	SIV$^+$ RM	2.88 ± 0.77	33 ± 19
Memory (CD95$^+$) subset	SIV$^-$ SM	3.66 ± 1.41	19 ± 10
	SIV$^+$ SM	2.08 ± 0.89	17 ± 8
	SIV$^-$ RM	4.76 ± 1.02	41 ± 14
	SIV$^+$ RM	4.24 ± 1.2	24 ± 14
Naïve (CD95$^-$) subset	SIV$^-$ SM	1.51 ± 0.98	12 ± 8
	SIV$^+$ SM	1.24 ± 1.25	2 ± 0.7
	SIV$^-$ RM	1.77 ± 0.5	25 ± 10
	SIV$^+$ RM	1.1 ± 0.56	8 ± 6

[a] PBMCs from 12 SIV$^-$ and 12 SIV$^+$ animals of each of the two primate species RM and SM were analyzed.

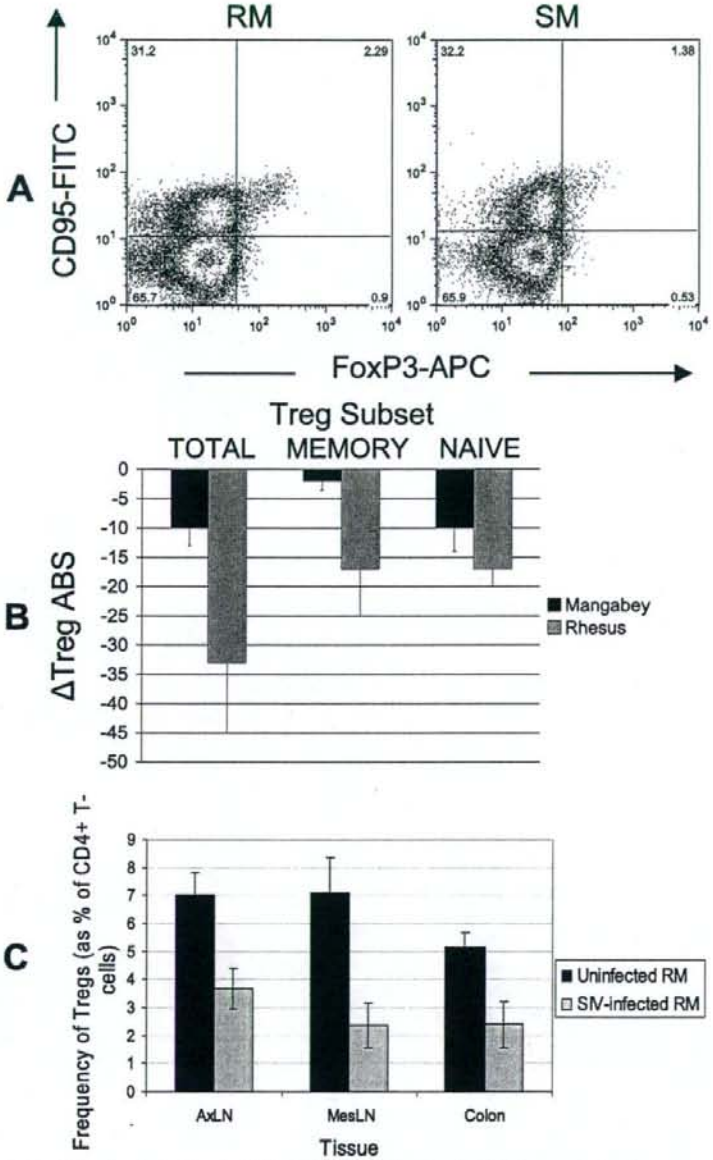

FIG. 2. Cross-sectional study of Treg levels in chronically SIV-infected SM and RM. (A) Representative flow cytometric profile illustrating the FoxP3$^+$ populations within memory (CD95$^+$) and naïve (CD95$^-$) CD4$^+$ subsets in RM (n = 12) and SM (n = 12). (B) Data obtained for uninfected monkeys were used to determine the change in ABS for each Treg subset in SIV-infected SM and RM. (C) The frequencies of Tregs (means ± SD) in the axillary lymph nodes (AxLN), mesenteric lymph nodes (MesLN), and colon were determined for uninfected (n = 5) and SIV-infected (n = 4) RM.

the in vitro suppression/MLR assays utilizing the CD4$^+$ CD25$^+$ subset (see below).

The ABS of peripheral Tregs decrease significantly in RM but not SM following SIV infection. To determine if the distinct clinical course and immune responses exhibited by SIV-infected RM and SM are due to differences in the levels of Tregs, a cross-sectional study was performed. PBMCs from 12 individual SIVmac239 chronically infected RM with relatively high VL (>100,000 copies of viral RNA [vRNA]/ml of plasma) and 12 naturally chronically SIV-infected (FUo viral isolate) SM with similar VL were analyzed for frequencies and ABS of Tregs. The frequencies of Tregs within the total CD4$^+$ popu-

lation and the $CD4^+$ memory and naïve subsets were determined. The cell surface marker CD95 was used to distinguish between memory ($CD95^+$) and naïve ($CD95^-$) subsets in RM and SM, as previously described (6, 42), and results are illustrated in Fig. 2A. Since CD4 T-cell levels changed dramatically over the course of infection, particularly in RM, it was reasoned that the data on frequency alone may not be an accurate reflection of true physiological changes. Therefore, the mean ABS of Tregs within each $CD4^+$ subset was also calculated; these data are summarized in Table 1. A feature common to both species is that the predominant frequency and ABS of Tregs appear in the memory $CD4^+$ T-cell subset (Table 1 and Fig. 2A). Conversely, if considering the total $CD25^{hi}$ $FoxP3^+$ Treg fraction, memory and naïve subsets are still distinguishable (flow cytometric profile not shown), with the majority of Tregs possessing a memory phenotype. The frequencies of $CD95^+$ $CD25^{hi}$ $FoxP3^+$ Tregs would typically range from 60 to 70% in both uninfected RM and SM (Table 1). The examination of $CD127^{lo}$ $FoxP3^+$ subsets revealed similar results (not shown).

A comparative analysis of the frequencies of Tregs in uninfected versus chronically infected animals showed a minor decline in frequency of Tregs in the total population and the naïve and memory subsets in both RM and SM. However, the analysis of ABS revealed a notable change in the level of Tregs exhibited by the chronically SIV-infected animals. As indicated in Fig. 2B, SIV-infected SM exhibited a minimal change in total Treg ABS ($P = 0.10$) while a clear significant decrease was observed in chronically SIV-infected RM ($P = 0.00026$). Although a decrease in the naïve Treg subset was observed in SIV-infected SM, normal levels of memory Treg levels were maintained. However, in SIV-infected RM the naïve and memory Treg subsets were threefold and twofold lower, respectively, than the levels in healthy uninfected RM. The decrease in ABS but not the frequency of Tregs in SIV-infected RM suggests that the decrease is not specific to the Treg subset but likely reflects the overall depletion of $CD4^+$ T cells that occurs over the course of SIV infection. A limited study of the frequencies of Tregs in the axillary lymph nodes, mesenteric lymph nodes, and colons from five uninfected and three SIVmac239-infected RM (obtained during autopsy) indicated that, following SIV infection, a decrease in Tregs also occurs in these major sites of infection, at least during the terminal stages of the disease (Fig. 2C). Additional testing of samples from other organs, such as the spleen and liver, and bronchoalveolar lavage specimens did not reveal any noticeable difference (data not shown). Thus, while the frequencies of peripheral Tregs remained relatively unchanged in both chronically SIV-infected SM and RM, these values masked the substantial decrease that occurred in the ABS of Tregs in SIV-infected RM and the maintenance of such cells in SIV-infected SM. Since the regulatory effect of Tregs depends largely on their ratio to memory T cells, this factor was also considered for uninfected and SIV-infected RM and SM. Results suggest a slight decrease in total Treg:memory $CD4^+$ T-cell ratio in SIV-infected RM (0.081 ± 0.029 to 0.06 ± 0.018; $P = 0.061$), while the decrease in the ratio in SIV-infected SM appeared to be statistically significant (0.056 ± 0.025 to 0.021 ± 0.012; $P = 0.038$). However, it is unclear if these are accurate representations of true cellular ratios, given the immense variability in the numbers of CD4 T cells following infection, particularly in the SM that were sampled.

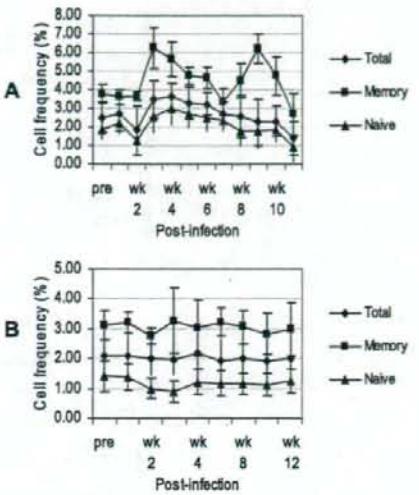

FIG. 3. Longitudinal study of Tregs during the acute phase of SIV infection in RM and SM. A total of 26 RM and three SM were experimentally infected intravenously with SIVmac239 and SM SIV isolate FUo, respectively, and the mean frequencies (±SD) of Tregs within the total $CD4^+$ population and within the memory and naïve $CD4^+$ T-cell subsets were determined by flow cytometry at the indicated time points from preinfection (pre) to 12 weeks (wk) p.i.

SIV-infected RM but not SIV-infected SM exhibit an increased Treg response during the acute phase of infection. Since there was a marked decrease in the ABS of Tregs in SIV-infected RM during the chronic-viremia period, it was important to determine the kinetics by which such a decrease occurs in this species and whether any changes could be observed during the same acute-infection period in SM. A longitudinal study was performed in which a total of 26 RM and, for comparison, three SM were monitored prior to and at weekly time intervals during the acute viremia phase following experimental infection with SIVmac239 or FUo viral isolates, respectively. Both species exhibited a peak in VL ($>10^6$ copies/ml) at ~2 weeks postinfection (p.i.), and the VL remained at or near this level (10^4 to 10^6 copies/ml) over the next 10 weeks of SIV infection (not shown). Figure 3A and B show the mean frequencies of total Tregs within the $CD4^+$ T-cell population and the mean frequencies of naïve and memory $CD4^+$ T cells that express the Treg phenotype in PBMC samples from SIV-infected RM and SM. As shown, the SIVmac239-infected RM showed a slight decrease in the frequency of total Tregs within the first 2 weeks of infection, reflecting the rapid decline in total CD4 T cells during this period of infection. This decline was followed by an ~2-fold increase in the frequency of Tregs at 3 weeks p.i., particularly within the memory subset; however, this sharp rise was not reflected by an increase in ABS, suggesting that a depletion of memory CD4 T cells other than Tregs contributed to this observation. Indeed, there was a larger decline in memory $CD4^+$ T cells (not shown), resulting in an overall doubling in the ratio of Tregs:$CD4^+$ T cells. Similarly, there appeared to be another increase in the fre-

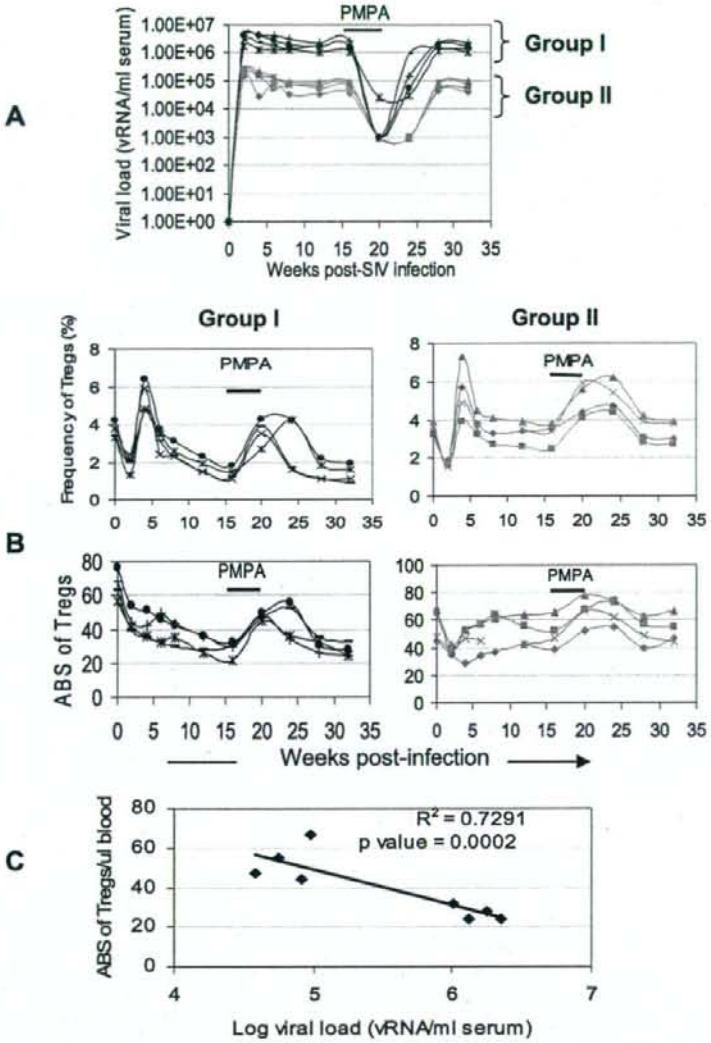

FIG. 4. Longitudinal study of the levels of peripheral Tregs during acute and chronic SIV infection in RM. A total of 26 RM were experimentally infected intravenously with SIVmac239. (A) Plasma VL and (B) frequencies and ABS of Tregs were determined over the course of infection. Data shown are for eight such animals, four with high VL and four with low VL. This group of animals was administered the nucleoside reverse transcriptase inhibitor PMPA at ~16 weeks p.i. (20 mg/kg daily for 30 days). (C) The correlation between VL and ABS of Tregs during the chronic phase was determined.

quency of Tregs within the memory $CD4^+$ subset at 9 weeks p.i., followed by a sharp decline in all Treg subsets. The frequency (Fig. 3B) and ABS (not shown) of Tregs in SIV-infected SM, on the other hand, remained generally unaltered during the first 12 weeks of infection.

Plasma VL and immune activation inversely correlate with the level of circulating Tregs in SIV-infected RM but not SIV-infected SM. The longitudinal analysis of Tregs in SIVmac239-infected RM following the acute phase revealed a recovery in the level of Tregs in a few of the animals, and a closer examination of these observations suggested that this resurgence in Tregs was related to a lower VL (Fig. 4). This finding prompted us to examine the data on the frequency and ABS of Tregs as a function of VL. The data were divided into two groups of SIV-infected RM, with one group exhibiting relatively high VL set points ($>10^5$ vRNA/ml serum) (group I) and the other displaying low VL set points ($<10^5$ vRNA/ml serum) (group II). Whereas similar trends were observed in both groups during the first 4 weeks of infection, a progressive decrease in the frequency and ABS of Tregs was observed for group I (high VL) while the ABS of Tregs in group II (low VL) began to recover after 4 weeks, with frequencies remaining

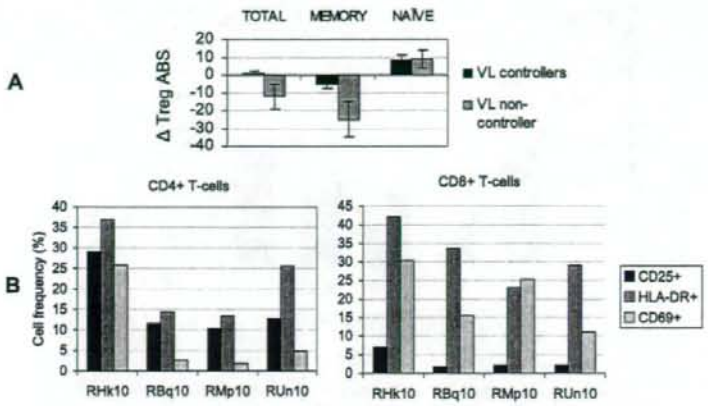

FIG. 5. Analysis of Treg levels and frequencies of activated cells in PBMCs from chronically SIV-infected RM (group III, $n = 3$) that spontaneously control VL in the absence of ART. Shown for comparison are data for PBMCs from monkey RHk10, an untreated SIV-infected RM with high VL. (A) The change in ABS of each Treg subset was determined ~8 months after experimental infection with SIVmac239. Means ± SD are shown. (B) The frequencies of $CD4^+$ and $CD8^+$ T cells expressing the activation markers CD25, CD69, and HLA-DR were determined. The RM with high VL is RHk10.

near baseline. Analysis by the linear-regression method and the Mann-Whitney test revealed a significant inverse correlation between the VL and ABS of Tregs during the chronic phase of infection (Fig. 4C) ($r^2 = 0.730$, $P = 0.0002$). In contrast, a similar comparison between VL and Tregs in 12 SIV-infected SM with low viremia and nine SIV-infected SM with high viremia revealed no correlation (data not shown).

As expected, treatment of both groups of RM with the nucleoside reverse transcriptase inhibitor PMPA (20 mg/kg) daily for 4 weeks resulted in a decline in viremia; an accompanying increase in the frequency and ABS of Tregs was also observed. This increase in Tregs was once again reflective of total CD4 T-cell levels. However, the VL in group I soon increased to high set point levels even before the completion of treatment, leading to a continued decline in the level of Tregs, while group II exhibited an increase in the frequency and ABS of Tregs that was maintained even after viremia returned to a lower set point. Analysis of Tregs in another group (group III) of three chronically SIV-infected RM (RBq10, RMp10, and RUn10) that spontaneously maintained low VL (less than 10^3 vRNA/ml serum) in the absence of ART revealed similar results (Fig. 5). Shown for comparison are results for the SIV-infected RM RHk10, which is representative of VL noncontrollers ($n = 3$) that were not provided ART. Data for this particular animal are shown since it was infected at the same time with the same inoculum as the other three VL controllers included in this experiment. Analysis of Tregs in PBMC samples from these RM prior to and approximately 32 weeks after SIV infection revealed that the loss of Tregs in VL noncontroller animals ($\Delta ABS = -25$) was significantly greater ($P < 0.05$) than that in the VL controllers ($\Delta ABS = -5$), with a particularly pronounced decline in the memory Treg subset (Fig. 5A). To determine if there was a correlation between this marked difference in Tregs and the state of immune activation, the expression levels of the activation markers CD25, CD69, and HLA-DR on $CD4^+$ and $CD8^+$ T cells were assessed. Indeed, the frequencies of activated $CD4^+$ and $CD8^+$ T cells in VL controllers were on average significantly lower than levels in the noncontrollers (Fig. 5B). These data indicate that recovery and/or maintenance of Tregs was associated with low plasma VL and low immune activation in chronically SIV-infected RM.

Treg function is maintained in chronically SIV-infected RM and SM. Although determining the frequency and VL of Tregs during SIV infection sheds some light on their role in SIV pathogenesis, it is equally important to assess the effect on SIV infection on Treg function. Tregs are characterized by their ability to suppress the activation and effector function of T cells predominantly by a contact-dependent mechanism (28, 32). To compare the inhibitory functions of Tregs in uninfected and SIV-infected SM and RM, two different assays were performed. In the first assay, CD25-depleted $CD4^+$ responder T cells from uninfected RM ($n = 9$) and SM ($n = 9$) were cocultured with a mixed pool of irradiated allogeneic PBMCs from RM and SM, respectively, in the absence (control) or presence of 1:1, 0.5:1, 0.25:1, and 0.125:1 autologous Tregs: CD25-depleted $CD4^+$ T cells. As seen in the representative profiles in Fig. 6A, Tregs from each of the two species appeared to decrease the *allo*-proliferative response. In efforts to determine whether there were differences in Treg activity, relative units of Tregs were calculated from such data. Thus, the number of Tregs that decreased the proliferative response by 33.3% was defined as 1 U of activity, which was then multiplied to derive the units of activity per million Tregs. The calculated Treg units of activity from one such data set were 9, 12, and 20 per million Tregs in three RM and 21, 31, and 38 per million Tregs in three SM and are representative of the three independent assays performed. These data suggest that there is perhaps increased functional Treg activity in uninfected SM compared to activity in uninfected RM; however, to confirm this observation an additional functional assay to further compare Tregs from uninfected and SIV-infected animals from the two species was performed. A limiting dilution assay was thus set up in which a fixed number of irradiated stimulators

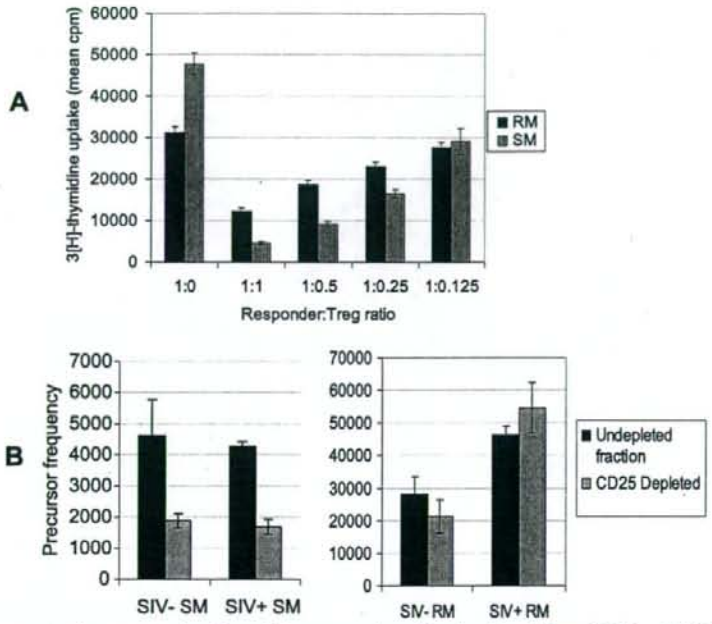

FIG. 6. In vitro MLR assay to demonstrate the effect of Tregs on cell proliferation in uninfected RM and SM. (A) Treg-depleted $CD4^+$ responder T cells were isolated from PBMCs from uninfected RM (n = 9) or SM (n = 9) and cocultured with a fixed number of allogeneic irradiated stimulators in the absence or presence of the indicated ratios of autologous Tregs. The *allo*-proliferative response was determined 5 days later by measuring ^{3}[H]thymidine uptake; shown for each species are data representative of at least three independent assays. (B) In vitro proliferation of undepleted and CD25-depleted PBMC fractions from SIV^- and SIV^+ SM (n = 10) and SIV^- and SIV^+ RM (n = 10) was determined by MLR assay. Responders (undepleted or CD25-depleted PBMC fractions) were incubated with irradiated stimulators in a 96-well plate for 5 days at 37°C and 5% CO_2. Sixteen hours prior to harvest, plates were pulsed with 1 μCi/well ^{3}[H]thymidine. Thymidine uptake was determined, and the precursor frequency was calculated. Data shown are means ± SD, representative of at least three independent assays.

were cocultured with a decreasing number of responder cells (PBMCs with or without Tregs) from uninfected (n = 10) and SIV-infected (n = 10) SM or RM with high VL. The minimum frequency of cells capable of *allo*-MLR response (precursor frequency) was determined. As illustrated by the representative data in Fig. 6B, CD25-depleted cell fractions from both uninfected and SIV-infected SM exhibited similar increases in MLR response, indicated by the ~60% decrease in precursor frequency (note that a decrease in the precursor value denotes an increased number of responding cells). A smaller decrease in precursor frequency (~25%) was noted for uninfected RM. However, no significant change was observed in PBMCs from SIV-infected RM. Collectively, these data therefore suggest that SM have increased functional Treg activity (compared to that for RM), which is maintained following SIV infection; however, not only do RM have a lower Treg functional activity but this functional activity is diminished during chronic infection.

The demonstration of Treg function in these assays prompted us to investigate the role of Tregs in the SIV-specific immune response in SM and RM. The in vitro $CD4^+$ T-cell response to SIV Env and Gag peptide pools was thus determined. PBMC samples from nine uninfected and 12 SIV-infected SM and RM were depleted of Tregs, and by use of immunofluorescent cell count the immune responses to eight pools of SIV Env peptides or eight pools of SIV Gag peptides were determined by measuring the frequencies of IFN-γ-producing $CD4^+$ T cells. Representative data from one animal from each of these two species are shown in Fig. 7. As expected, while $CD4^+$ T cells from both species exhibited a minimal response to the Ova peptide (negative control), concanavalin A and tetanus toxoid induced an increased IFN-γ response, which was markedly increased by the depletion of Tregs. The $CD4^+$ T cells from the SIV-negative RM and SM, also as expected, failed to show any IFN-γ response when tested against a panel of SIV env and gag peptide pools. Of importance was the finding that select pools of SIV env and gag peptides induced IFN-γ production in PBMCs from the SIV-infected RM (Fig. 7, top) and the frequency of responding cells increased significantly (≥2-fold) in the CD25-depleted fractions (Fig. 7, top). In contrast, not only did the $CD4^+$ T cells from the SIV-infected SM fail to respond, removal of the $CD4^+$ $CD25^+$ T cells from an aliquot of the same PBMCs prior to the assay consistently failed to show any detectable increase in the responses (Fig. 7, bottom). Similar results were obtained for the $CD8^+$ T-cell response (data not shown). Thus, the presence of Tregs in PBMCs from RM and SM clearly regulates the magnitude of antigen-specific responses. However, while Tregs from SIV-infected RM dampened the virus-specific T-cell response to select SIV peptides in vitro, the removal of Tregs did not lead to any detectable SIV-specific cellular responses in SIV-infected SM, making it difficult to

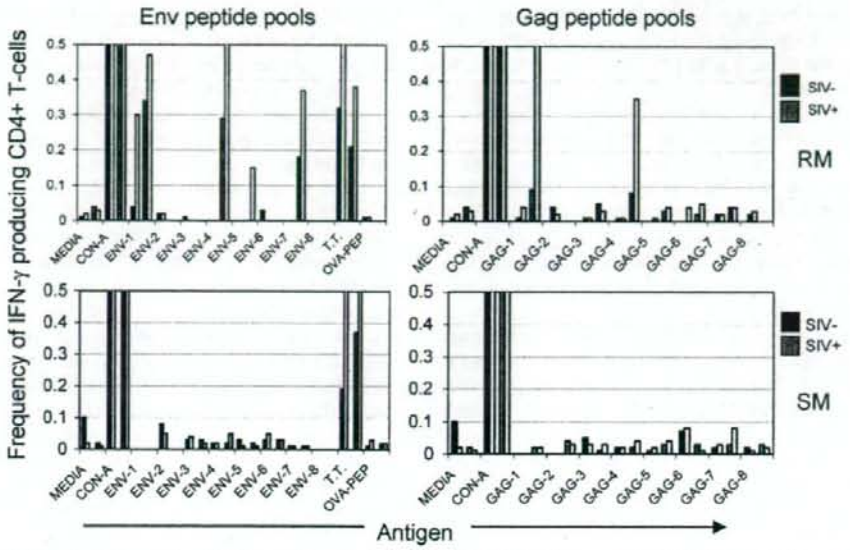

FIG. 7. Effect of Treg depletion on the SIV Env or Gag peptide-specific $CD4^+$ T-cell response in PBMCs from SIV^- or SIV^+ RM and SM. Shown are unfractionated PBMCs from SIV^- and SIV^+ animals (black and gray bars, respectively) that are paired with their corresponding $CD4^+CD5^+$ T-cell-depleted fraction (white bars). Cells were cultured in the presence of concanavalin A (CON-A) (polyclonal positive control), Ova (OVA-PEP) (negative control), tetanus toxoid (T.T.) (antigen-specific positive control), and eight Env or Gag peptide pools in the presence of brefeldin A. Cells were surface stained for CD4 and then fixed/permeabilized and stained to detect IFN-γ. The frequency of IFN-γ-producing $CD4^+$ T cells was determined by flow cytometry. Shown are data representative of 12 animals of each species. Similar data were obtained for $CD8^+$ T-cell responses (data not shown).

comment on the role of this cell lineage in the virus-specific immune response in the SM species, at least with the pools of peptides that were utilized in this assay.

DISCUSSION

Support for a role of Tregs in HIV disease progression has kindled interest in defining whether such a role is also present in the SIV-infected nonhuman primate models of AIDS. The rationale here is that a more definitive assignment of a role for this cell lineage in lentiviral infection can be made only by using in vivo manipulative studies of this cell lineage, which is not deemed practical with HIV-infected humans. This determined the purpose of the studies reported herein. Studies with HIV-infected humans thus far have shown that a relative increase in the frequency of Tregs appears to correlate with lower plasma VL and slower disease progression (1, 11, 22, 30). The hypothesis was that Tregs function to regulate the generation of activated $CD4^+$ T cells, which indirectly leads to lower target cells in which the virus could infect and replicate (15, 16, 46), contributing to lower VL and slower disease progression. The main objective of the present study was to identify reagents that would identify Tregs in nonhuman primates, to characterize and compare the levels and functions of Tregs in uninfected and SIV-infected RM and SM, and to determine if observed differences related to the polarized immune responses over the course of infection in these two species. While it is well recognized that immune control is exerted by a number of Treg subsets (natural versus adaptive), such as Tr1, Th3, Th17, and even $CD8^+$ Tregs, the focus of the studies reported herein was the natural $CD4^+$ $CD25^+$ $FoxP3^+$ Tregs that generally develop in the thymus during the early stages of fetal and neonatal T-cell development. It is important to note that the peripheral expansion of $FoxP3^+$-adaptive Tregs has also been suggested previously (7, 8, 19, 36). The characterization of Tregs described here is therefore likely to represent both natural and adaptive subsets of Tregs.

The examination of the kinetics of Tregs during the acute-infection period in RM and SM revealed that divergent Treg responses are exhibited early on by these two species, which may be a critical factor influencing disease outcome. A decrease in the ABS of Tregs occurred during the acute phase in SIV-infected RM, but a larger decline in memory CD4 T cells within the first 3 weeks resulted in a larger Treg:CD4 ratio. A similar trend occurred at 9 weeks p.i., presumably due to the depletion and/or redistribution of memory CD4 T cells. This overall premature Treg induction in SIV-infected RM, which is in agreement with results from a recent study (13), may result in the downregulation of effector T-cell responses at a time when immune control and viral clearance are most important. It may also contribute to an early exhaustion of the generative potential and/or function of Tregs that would be crucial for the prevention or regulation of chronic immune hyperactivation that ultimately results from the persistent viral infection. There was no change in the level of Tregs in SIV-infected SM during the acute phase, and the absence of an early Treg response is in contrast to the rapid immunosuppressive response exhibited by African green monkeys, another natural host of SIV that does not develop AIDS. However, the interpretation of data

from this study is an issue at present since the study was based on characterizing Tregs using the expression of FoxP3 at the message but not the protein level (23). The Treg induction in African green monkeys occurred even earlier than in RM, and it was suggested that this immediate response, although too early to prevent viral replication, may be adequate to prevent chronic immune activation in later stages of infection. In SIV-infected SM, the lack of an early pronounced Treg response may conserve immunological resources necessary for an effective sustained Treg-mediated regulation over the course of infection. It may also be possible that an early Treg induction did occur during the first week of infection prior to our analysis at the 7-day time point.

The analysis of Tregs in animals from the longitudinal study revealed a progressive decline in this cell subset in SIV-infected RM with high plasma VL, but no such decrease occurred in SIV-infected SM. These results were consistent with data from the cross-sectional study, and the decline in Tregs was even more dramatic in the late chronic stage of infection, with the frequency and ABS of Tregs as low as 1.40% ± 1.15% and 2.0% ± 1.4%, respectively. This was also supported by the marked decreases seen in the peripheral and gut-associated lymph node tissues (Fig. 2C). This decline is not unexpected given that the majority of Tregs possess a memory phenotype and a high proportion of this subset expresses CCR5 (L. Picker, unpublished data), the coreceptor used by the virus for cell entry. Thus, the depletion of Tregs over the course of infection is a reflection of the decline in the overall memory CD4 T-cell population, as described before (11, 17, 22). The decline in Tregs could also be attributed to a decrease in CD28 expression following SIV infection (data not shown) since CD28-mediated costimulatory signals have been implicated in the thymic development and peripheral homeostasis of Tregs (44). In contrast to the observed decline in peripheral Tregs in SIV-infected RM, the ABS of Tregs in chronically SIV-infected SM was generally unaltered. It would therefore appear that the chronic immune hyperactivation characteristic of SIV-infected RM might be partly due to the loss of Tregs. In support of this hypothesis, a higher number of Tregs was associated with a lower level of immune activation in chronically SIV-infected RM (Fig. 5). In addition to the observed relationship between Tregs and immune activation, an inverse correlation between Tregs and plasma VL was noted to occur during the chronic state of infection. SIV-infected RM with high VL were found to exhibit higher levels of immune activation and lower numbers of Tregs. This elevated state of activation would provide additional target cells that would further sustain a high VL. Although the observed correlation suggests that high levels of immune activation and VL are a consequence of a decline in Tregs, the data also support the notion that the decrease in Tregs is a consequence of the overall decline in the general CD4 T-cell population due to viral pathogenesis. Indeed, the ability of SIV-infected SM and RM VL controllers to retain Tregs was reflected by the maintenance in total CD4 T cells, and a correlation between the level of Tregs and total CD4 T cells was noted (not shown), in agreement with a recent study involving SM (42). Thus, Tregs may contribute to CD4 T-cell preservation due to its inhibitory effect on immune activation. Conversely, the decline in Tregs in RM VL noncontrollers as a result of viral pathogenesis may be a factor contributing to high levels of immune activation, perpetuating the cycle of viral replication, cell activation, and cell death. Although the data presented herein suggest a positive role for Tregs in SIV infection and/or disease progression, a potential detrimental effect of Tregs via an influence on crucial antiviral immune responses cannot be ruled out. The key to the successful control of viral replication and/or disease progression may perhaps be related to the infection stage at which Tregs exert their regulatory effect, and of course the contribution of other Treg subsets cannot be overlooked.

The decline in the number of Tregs in SIV-infected RM that is suggested by our data does not rule out the effect of SIV-mediated alteration or disruption of Treg function. To address this issue, we first compared the suppressive activities of Tregs isolated from uninfected and SIV-infected SM and RM. In vitro MLR assays suggest that Tregs from uninfected SM generally exhibit a greater degree of suppression than those from RM, and while this potency was maintained in SIV-infected SM, there appeared to be a loss in Treg-mediated suppression in SIV-infected RM. However, the modest enhancement in the response of CD25-depleted cell fractions from SIV-infected RM to select SIV peptide pools suggests that while this cell subset is still functional it most likely plays a limited regulatory role in SIV pathogenesis. Our results therefore suggest that it may be the decline in the number of Tregs and not their loss in function that contributes to the excessive SIV-specific immune response in SIV-infected RM. Since no distinct in vitro response to SIV peptides was observed for PBMCs from SIV-infected SM, which is in agreement with results from a previous study (10), it is difficult to comment on the role of Tregs in the SIV-specific immune response in this species. However, responses to tetanus toxoid were clearly enhanced in the CD25-depleted PBMC fraction, providing support to the notion that the failure was not secondary to a technical issue. In addition, it is important to keep in mind that the SIV peptides being utilized to study the SIV-specific immune response in the SM are based on the SIVmac239 sequence, which may be represented poorly in SM. A more intense study of the effect of SIV infection on Treg function in these animal models, using in vivo depletion of this subset, is under way in our laboratory.

In summary, the present study involved the phenotypic and functional characterization of Tregs from SM and RM and the impact of SIV infection on these parameters. Results show a decline in peripheral Tregs in SIV-infected RM, and the extent of this depletion was found to inversely correlate with both plasma VL and immune activation. In addition to affecting the level of Tregs, SIV infection in RM appears to have a negative impact on Treg function. Thus, while Tregs may contribute to the control of immune activation and VL in RM, the observed trends may simply be attributed to viral pathogenesis. Therefore, the exact nature of this relationship remains to be elucidated. In contrast, both the frequency and the function of Tregs are maintained in SIV-infected SM, leaving their role in disease resistance currently unresolved. Since the regulatory impact of Tregs ultimately depends on their stoichiometry to $CD4^+$ and perhaps total $CD3^+$ effector T cells, a closer examination of the ratio of Tregs to these T-cell populations in both the periphery and the major sites of infection would provide additional insight into the role of Tregs in SIV pathogenesis. The positive effect of ART on Tregs in SIV-infected RM that

is suggested by our data is promising and encourages the design of therapeutic strategies to aid Treg development and/or survival that would limit the immune system damage characteristic of SIV/HIV infection. A recent study suggests that cytotoxic-T-lymphocyte-associated antigen 4 blockade on Tregs in conjunction with ART further reduces vRNA expression in tissues and that this was associated with an increase in virus-specific effector immune responses (but not cell activation, which would favor viral replication) (18). Thus, in addition to increasing Treg levels by using ART, other immune strategies can be employed. It is unclear if the increase in peripheral Tregs observed during ART is a true expansion, a result of T-cell redistribution, or both. The potent immunosuppressive cytokine TGF-β has previously been reported to induce the expression of FoxP3 in $CD4^+$ $CD25^-$ T cells, conferring suppressive activity (8, 14) and possibly thus contributing to Treg development and/or survival. Although previous studies have reported TGF-β induction during the acute phase of SIV infection (13, 23), it would be of interest to assess how TGF-β profiles compare to Treg dynamics over the entire course of infection, particularly in hosts that control VL and do not progress to disease. Analysis of homing markers, such as CCR7 and $\alpha_4\beta_1/\beta_7$ integrins, may address the alternative issue of Treg redistribution.

ACKNOWLEDGMENTS

This work was supported by NIH RO1 27057 and by AIDS research grants from the Health Sciences Research Grants from the Ministry of Health, Labor and Welfare in Japan.

We are indebted to M. Miller and Gilead Sciences (Foster City, CA) for their generous gift of PMPA for use in these studies.

REFERENCES

1. **Aandahl, E. M., J. Michaelsson, W. J. Moretto, F. M. Hecht, and D. F. Nixon.** 2004. Human $CD4^+$ $CD25^+$ regulatory T cells control T-cell responses to human immunodeficiency virus and cytomegalovirus antigens. J. Virol. **78:**2454–2459.
2. **Annacker, O., R. Pimenta-Araujo, O. Burlen-Defranoux, T. C. Barbosa, A. Cumano, and A. Bandeira.** 2001. CD25+ CD4+ T cells regulate the expansion of peripheral CD4 T cells through the production of IL-10. J. Immunol. **166:**3008–3018.
3. **Apoil, P. A., B. Puissant, F. Roubinet, M. Abbal, P. Massip, and A. Blancher.** 2005. FoxP3 mRNA levels are decreased in peripheral blood CD4+ lymphocytes from HIV-positive patients. J. Acquir. Immune Defic. Syndr. **39:** 381–385.
4. **Baecher-Allan, C., J. A. Brown, G. J. Freeman, and D. A. Hafler.** 2001. CD4+CD25high regulatory cells in human peripheral blood. J. Immunol. **167:**1245–1253.
5. **Baecher-Allan, C., E. Wolf, and D. A. Hafler.** 2005. Functional analysis of highly defined, FACS-isolated populations of human regulatory CD4+CD25+ T cells. Clin. Immunol. **115:**10–18.
6. **Bostik, P., E. S. Noble, A. E. Mayne, L. Gargano, F. Villinger, and A. A. Ansari.** 2006. Central memory CD4 T cells are the predominant cell subset resistant to anergy in SIV disease resistant sooty mangabeys. AIDS **20:**181–188.
7. **Chatenoud, L., and J. F. Bach.** 2006. Adaptive human regulatory T cells: myth or reality? J. Clin. Investig. **116:**2325–2327.
8. **Chen, W., W. Jin, N. Hardegen, K. J. Lei, L. Li, N. Marinos, G. McGrady, and S. M. Wahl.** 2003. Conversion of peripheral CD4+CD25− naive T cells to CD4+CD25+ regulatory T cells by TGF-beta induction of transcription factor Foxp3. J. Exp. Med. **198:**1875–1886.
9. **Cobb, B. S., A. Hertweck, J. Smith, E. O'Connor, D. Graf, T. Cook, S. T. Smale, S. Sakaguchi, F. J. Livesey, A. G. Fisher, and M. Merkenschlager.** 2006. A role for Dicer in immune regulation. J. Exp. Med. **203:**2519–2527.
10. **Dunham, R., P. Pagliardini, S. Gordon, B. Sumpter, J. Engram, A. Moanna, M. Paiardini, J. N. Mandl, B. Lawson, S. Garg, H. M. McClure, Y. X. Xu, C. Ibegbu, K. Easley, N. Katz, I. Pandrea, C. Apetrei, D. L. Sodora, S. I. Staprans, M. B. Feinberg, and G. Silvestri.** 2006. The AIDS resistance of naturally SIV-infected sooty mangabeys is independent of cellular immunity to the virus. Blood **108:**209–217.
11. **Eggena, M. P., B. Barugahare, N. Jones, M. Okello, S. Mutalya, C. Kityo, P. Mugyenyi, and H. Cao.** 2005. Depletion of regulatory T cells in HIV infection is associated with immune activation. J. Immunol. **174:**4407–4414.
12. **Epple, H. J., C. Loddenkemper, D. Kunkel, H. Troger, J. Maul, V. Moos, E. Berg, R. Ullrich, J. D. Schulzke, H. Stein, R. Duchmann, M. Zeitz, and T. Schneider.** 2006. Mucosal but not peripheral FoxP3+ regulatory T cells are highly increased in untreated HIV infection and normalize after suppressive HAART. Blood **108:**3072–3078.
13. **Estes, J. D., Q. Li, M. R. Reynolds, S. Wietgrefe, L. Duan, T. Schacker, L. J. Picker, D. I. Watkins, J. D. Lifson, C. Reilly, J. Carlis, and A. T. Haase.** 2006. Premature induction of an immunosuppressive regulatory T cell response during acute simian immunodeficiency virus infection. J. Infect. Dis. **193:** 703–712.
14. **Fantini, M. C., C. Becker, G. Monteleone, F. Pallone, P. R. Galle, and M. F. Neurath.** 2004. Cutting edge: TGF-beta induces a regulatory phenotype in CD4+CD25− T cells through Foxp3 induction and down-regulation of Smad7. J. Immunol. **172:**5149–5153.
15. **Finzi, D., M. Hermankova, T. Pierson, L. M. Carruth, C. Buck, R. E. Chaisson, T. C. Quinn, K. Chadwick, J. Margolick, R. Brookmeyer, J. Gallant, M. Markowitz, D. D. Ho, D. D. Richman, and R. F. Siliciano.** 1997. Identification of a reservoir for HIV-1 in patients on highly active antiretroviral therapy. Science **278:**1295–1300.
16. **Finzi, D., and R. F. Siliciano.** 1998. Viral dynamics in HIV-1 infection. Cell **93:**6314–6319.
17. **Grossman, Z., M. Meier-Schellersheim, W. E. Paul, and L. J. Picker.** 2006. Pathogenesis of HIV infection: what the virus spares is as important as what it destroys. Nat. Med. **12:**289–295.
18. **Hryniewicz, A., A. Boasso, Y. Edghill-Smith, M. Vaccari, D. Fuchs, D. Venzon, J. Nacsa, M. R. Betts, W. P. Tsai, J. M. Heraud, B. Beer, D. Blanset, C. Chougnet, I. Lowy, G. M. Shearer, and G. Franchini.** 2006. CTLA-4 blockade decreases TGF-β, IDO and viral RNA expression in tissues of SIVmac251-infected macaques. Blood **108:**3834–3842.
19. **Itoh, M., T. Takahashi, N. Sakaguchi, Y. Kuniyasu, J. Shimizu, F. Otsuka, and S. Sakaguchi.** 1999. Thymus and autoimmunity: production of CD25+CD4+ naturally anergic and suppressive T cells as a key function of the thymus in maintaining immunologic self-tolerance. J. Immunol. **162:** 5317–5326.
20. **Jonuleit, H., E. Schmitt, M. Stassen, A. Tuettenberg, J. Knop, and A. H. Enk.** 2001. Identification and functional characterization of human CD4(+)CD25(+) T cells with regulatory properties isolated from peripheral blood. J. Exp. Med. **193:**1285–1294.
21. **Kaur, A., R. M. Grant, R. E. Means, H. McClure, M. Feinberg, and R. P. Johnson.** 1998. Diverse host responses and outcomes following simian immunodeficiency virus SIVmac239 infection in sooty mangabeys and rhesus macaques. J. Virol. **72:**9597–9611.
22. **Kinter, A. L., M. Hennessey, A. Bell, S. Kern, Y. Lin, M. Daucher, M. Planta, M. McGlaughlin, R. Jackson, S. F. Ziegler, and A. S. Fauci.** 2004. CD25(+)CD4(+) regulatory T cells from the peripheral blood of asymptomatic HIV-infected individuals regulate CD4(+) and CD8(+) HIV-specific T cell immune responses in vitro and are associated with favorable clinical markers of disease status. J. Exp. Med. **200:**331–343.
23. **Kornfield, C., M. J. Y. Ploquin, I. Pandrea, A. Faye, R. Onanga, C. Apetrei, V. Poaty-Mavoungou, P. Rouquet, J. Estaquier, L. Mortara, J. F. Desoutter, C. Butor, R. L. Grand, P. Roques, F. Simon, F. Barre-Sinoussi, O. M. Diop, and M. C. Muller-Trutwin.** 2005. Antiinflammatory profiles during primary SIV infection in African green monkeys are associated with protection against AIDS. J. Clin. Investig. **115:**1082–1091.
24. **Kuroda, M. J., J. E. Schmitz, W. A. Charini, C. E. Nickerson, M. A. Lifton, C. I. Lord, M. A. Forman, and N. L. Letvin.** 1999. Emergence of CTL coincides with clearance of virus during primary simian immunodeficiency virus infection in rhesus monkeys. J. Immunol. **162:**5127–5133.
25. **Levings, M. K., R. Sangregorio, and M. G. Roncarolo.** 2001. Human CD25+CD4+ T regulatory cells suppress naive and memory T-cell proliferation and can be expanded *in vitro* without loss of function. J. Exp. Med. **193:**1295–1302.
26. **Liu, W., A. L. Putnam, Z. Xu-Yu, G. L. Szot, M. R. Lee, S. Zhu, P. A. Gottlieb, P. Kapranov, T. R. Gingeras, B. F. D. St. Groth, C. Clayberger, D. M. Soper, S. F. Ziegler, and J. A. Bluestone.** 2006. CD127 expression inversely correlates with FoxP3 and suppressive function of human CD4+ T reg cells. J. Exp. Med. **203:**1701–1711.
27. **McHugh, R. S., M. J. Whitters, C. A. Piccirillo, D. A. Young, E. M. Shevach, M. Collins, and M. C. Byrne.** 2002. CD4(+)CD25(+) immunoregulatory T cells: gene expression analysis reveals a functional role for the glucocorticoid-induced TNF receptor. Immunity **16:**311–323.
28. **Nakamura, K., A. Kitani, and W. Strober.** 2001. Cell contact-dependent immunosuppression by CD4(+)CD25(+) regulatory T cells is mediated by cell surface-bound transforming growth factor beta. J. Exp. Med. **194:**629–644.

28a. **National Research Council.** 1996. Guide for the care and use of laboratory animals. National Academy Press, Washington, DC.

29. **Nilsson, J., A. Boasso, P. A. Velilla, R. Zhang, M. Vaccari, G. Franchini, G. M. Shearer, J. Andersson, and C. Chougnet.** 2006. HIV-1 driven regula-

tory T-cell accumulation in lymphoid tissues is associated with disease progression in HIV/AIDS. Blood **108:**3808–3817.
30. **Nixon, D. F., E. M. Aandahl, and J. Michaelsson.** 2005. CD4+CD25+ regulatory T cells in HIV infection. Microbes Infect. **7:**1063–1065.
31. **Oida, T., L. Xu, H. L. Weiner, A. Kitani, and W. Strober.** 2006. TGF-beta-mediated suppression by CD4+CD25+ T cells is facilitated by CTLA-4 signaling. J. Immunol. **177:**2331–2339.
32. **Piccirillo, C. A., J. J. Letterio, A. M. Thornton, R. S. McHugh, M. Mamura, H. Mizuhara, and E. M. Shevach.** 2002. CD4(+)CD25(+) regulatory T cells can mediate suppressor function in the absence of transforming growth factor beta1 production and responsiveness. J. Exp. Med. **196:**237–246.
33. **Rey-Cuille, M. A., J. L. Berthier, M. C. Bomsel-Demontoy, Y. Chaduc, L. Montagnier, A. G. Hovanessian, and L. A. Chakrabarti.** 1998. Simian immunodeficiency virus replicates to high levels in sooty mangabeys without inducing disease. J. Virol. **72:**3872–3886.
34. **Reynolds, M. R., E. Rakasz, P. J. Skinner, C. White, K. Abel, Z. M. Ma, L. Compton, G. Napoe, N. Wilson, C. J. Miller, A. Haase, and D. I. Watkins.** 2005. $CD8^+$ T-lymphocyte response to major immunodominant epitopes after vaginal exposure to simian immunodeficiency virus: too late and too little. J. Virol. **79:**9228–9235.
35. **Roncador, G., P. J. Brown, L. Maestre, S. Hue, J. L. Martinez-Torrecuadrada, K. L. Ling, S. Pratap, C. Toms, B. C. Fox, V. Cerundolo, F. Powrie, and A. H. Banham.** 2005. Analysis of FoxP3 protein expression in human CD4+CD25+ regulatory T cells at the single-cell level. Eur. J. Immunol. **35:**1681–1691.
36. **Sakaguchi, N.** 2005. Naturally arising Foxp3-expressing CD25+CD4+ regulatory T cells in immunologic tolerance to self and non-self. Nat. Immunol. **6:**345–352.
37. **Seddiki, N., B. Santner-Nanan, J. Martinson, J. Zaunders, S. Sasson, A. Landay, M. Solomon, W. Selby, S. I. Alexander, R. Nanan, A. Kelleher, and B. F. D. St. Groth.** 2006. Expression of interleukin (IL)-2 and IL-7 receptors discriminates between human regulatory and activated T cells. J. Exp. Med. **203:**1693–1700.
38. **Silvestri, G., A. Fedanov, S. Germon, N. Kozyr, W. J. Kaiser, D. A. Garber, H. McClure, M. B. Feinberg, and S. I. Staprans.** 2005. Divergent host responses during primary simian immunodeficiency virus SIVsm infection of natural sooty mangabey and nonnatural rhesus macaque hosts. J. Virol. **79:**4043–4054.
39. **Silvestri, G., D. L. Sodora, R. A. Koup, M. Paiardini, S. P. O'Neil, H. M. McClure, S. I. Staprans, and M. B. Feinberg.** 2003. Nonpathogenic SIV infection of sooty mangabeys is characterized by limited bystander immunopathology despite chronic high-level viremia. Immunity **18:**441–452.
40. **Strijbosch, L. W. G., R. J. M. M. Does, and W. A. Buurman.** 1988. Computer-aided design and evaluation of limiting and serial dilution experiments. Int. J. Biomed. Comput. **23:**279–290.
41. **Sugimoto, N., T. Oida, K. Hirota, K. Nakamura, T. Nomura, T. Uchiyama, and S. Sakaguchi.** 2006. FoxP3-dependent and -independent molecules specific for CD25+CD4+ natural regulatory T cells revealed by DNA microarray analysis. Int. Immunol. **18:**1197–1209.
42. **Sumpter, B., R. Dunham, S. Gordon, J. Engram, M. Hennessy, A. Kinter, M. Paiardini, B. Cervasi, N. Klatt, H. McClure, J. M. Milush, S. Staprans, D. L. Sodora, and G. Silvestri.** 2007. Correlates of preserved CD4+ T cell homeostasis during natural, nonpathogenic simian immunodeficiency virus infection of sooty mangabeys: implications for AIDS pathogenesis. J. Immunol. **178:**1680–1691.
43. **Takahashi, T., T. Tagami, S. Yamakazi, T. Uede, J. Shimizu, N. Sakaguchi, T. W. Mak, and S. Sakaguchi.** 2000. Immunological self-tolerance maintained by CD25(+)CD4(+) regulatory T cells constitutively expressing cytotoxic T lymphocyte-associated antigen 4. J. Exp. Med. **192:**303–310.
44. **Tang, Q., K. J. Henriksen, E. K. Boden, A. J. Tooley, J. Ye, S. K. Subudhi, X. X. Zheng, T. B. Strom, and J. A. Bluestone.** 2003. Cutting edge: CD28 controls peripheral homeostasis of CD4+CD25+ regulatory T-cells. J. Immunol. **171:**3348–3352.
45. **Tsunemi, S., T. Iwasaki, T. Imado, S. Higasa, E. Kakishita, T. Shirasaka, and H. Sano.** 2005. Relationship of CD4+CD25+ regulatory T cells to immune status in HIV-infected patients. AIDS **19:**879–886.
46. **Veazey, R. S., I. C. Tham, K. G. Mansfield, M. DeMaria, A. E. Forand, D. E. Shvetz, L. V. Chalifoux, P. K. Sehgal, and A. A. Lackner.** 2000. Identifying the target cell in primary simian immunodeficiency virus (SIV) infection: highly activated memory $CD4^+$ T cells are rapidly eliminated in early SIV infection in vivo. J. Virol. **74:**57–64.
47. **Weiss, L., V. Donkova-Petrini, L. Caccavelli, M. Balbo, C. Carbonneil, and Y. Levy.** 2004. Human immunodeficiency virus-driven expansion of CD4+CD25+ regulatory T cells, which suppress HIV-specific CD4 T-cell responses in HIV-infected patients. Blood **104:**3249–3256.
48. **Yagi, H., T. Nomura, K. Nakamura, S. Yamakazi, T. Kitawaki, S. Hori, M. Maeda, M. Onodera, T. Uchiyama, S. Fujii, and S. Sakaguchi.** 2004. Crucial role of FOXP3 in the development and function of human CD25+CD4+ regulatory T cell. Int. Immunol. **16:**1643–1656.

Journal of General Virology (2008), **89**, 554–566 DOI 10.1099/vir.0.83186-0

Impact of glycosylation on antigenicity of simian immunodeficiency virus SIV239: induction of rapid V1/V2-specific non-neutralizing antibody and delayed neutralizing antibody following infection with an attenuated deglycosylated mutant

Chie Sugimoto,[1,2,3] Emi E. Nakayama,[4] Tatsuo Shioda,[4] Francois Villinger,[5] Aftab A. Ansari,[5] Naoki Yamamoto,[1] Yasuo Suzuki,[3,6] Yoshiyuki Nagai[7] and Kazuyasu Mori[1,2,3]

Correspondence
Kazuyasu Mori
mori@nih.go.jp

[1]AIDS Research Center, National Institute of Infectious Diseases, Shinjuku-ku, Tokyo 162-8640, Japan

[2]Tsukuba Primate Research Center, National Institute of Biomedical Innovation, Tsukuba, Ibaraki 305-0843, Japan

[3]CREST, Japan Science and Technology Agency, Kawaguchi, Saitama 332-0012, Japan

[4]Department of Viral Infections, Research Institute for Microbial Diseases, Osaka University, Suita, Osaka 565-0871, Japan

[5]Department of Pathology and Laboratory Medicine, Emory University, Atlanta, GA 30322, USA

[6]Department of Biomedical Sciences, College of Life and Health Sciences, Chubu University, Kasugai, Aichi 487-8501, Japan

[7]Center of Research Network for Infectious Diseases, Riken, Chiyoda-ku, Tokyo 100-0006, Japan

Infection of rhesus macaques with a deglycosylation mutant, Δ5G, derived from SIV239, a pathogenic clone of simian immunodeficiency virus (SIV), led to robust acute-phase viral replication followed by a chronic phase with undetectable viral load. This study examined whether humoral responses in Δ5G-infected animals played any role in the control of infection. Neutralizing antibodies (nAbs) were elicited more efficiently in Δ5G-infected animals than in SIV239-infected animals. However, functional nAb measured by 90% neutralization was prominent in only two of the five Δ5G-infected animals, and only at 8 weeks post-infection (p.i.), when viral loads were already below 10^4 copies ml^{-1}. These results suggest a minimal role for nAbs in the control of the primary infection. In contrast, whilst Ab responses to epitopes localized to the variable loops V1/V2 were detected in all Δ5G-infected animals at 3 weeks p.i., this response was associated with a concomitant reduction in Ab responses to epitopes in gp41 compared with those in SIV239-infected animals. These results suggest that the altered surface glycosylation and/or conformation of viral spikes induce a humoral response against SIV that is distinct from the response induced by SIV239. More interestingly, whereas V1/V2-specific Abs were induced in all animals, these Abs were associated with vigorous Δ5G-specific virion capture ability in only two Δ5G-infected animals that exhibited a functional nAb response. Thus, whereas the deglycosylation mutant infection elicited early virion capture and subsequent nAbs, the responses differed among animals, suggesting the existence of host factors that may influence the functional humoral responses against human immunodeficiency virus/SIV.

Received 25 May 2007
Accepted 7 October 2007

INTRODUCTION

The precise role of antibody (Ab) responses in the containment of human immunodeficiency virus (HIV) remains a subject of intense study and debate. Besides the classical direct virus neutralization properties, antibodies are also capable of blocking infection via other pathways such as antibody-dependent complement-mediated inactivation of virus (Aasa-Chapman *et al.*, 2005) and antibody-dependent cellular lysis (Ahmad & Menezes, 1996; Forthal *et al.*, 2001). Acquiring an understanding of these various mechanisms for their exploitation in the

0008-3186 © 2008 SGM *Printed in Great Britain*

development of candidate vaccines has been a major challenge.

The envelope protein (Env) of HIV/simian immunodeficiency virus (SIV) comprises an exterior protein (gp120) and a transmembrane (TM) protein (gp41), and trimers of the gp120/gp41 complexes form viral spikes that promote binding to receptors and co-receptors on the cell membrane for entry into the target cells (Wyatt & Sodroski, 1998). The major viral receptors of HIV/SIV include CD4 and a variety of co-receptors such as CCR5 or CXCR4. One desirable target epitope for neutralizing antibody (nAb) that shows relative conservation across clades is the binding site for the co-receptor (Burton *et al.*, 2004; Zolla-Pazner, 2004); however, this site is conformationally cryptic within the viral spike up until immediately after binding of the viral spike to CD4, providing an effective shielding mechanism to the virus. Another distinct feature of HIV/SIV Env is the extensive glycosylation that also effectively prevents access to antibodies directed at the epitopes (Chen *et al.*, 2005; Wyatt & Sodroski, 1998; Wyatt *et al.*, 1998). The gp120 protein possesses 18–33 Asn–X–Ser/Thr sequences, signals for the attachment of *N*-linked carbohydrate side chains (Leonard *et al.*, 1990; Ohgimoto *et al.*, 1998; Regier & Desrosiers, 1990; Zhang *et al.*, 2004). As the carbohydrate moiety is generally weakly immunogenic and is recognized to a large extent as self by the host immune system, the massive glycans on the surface of viral spikes constitute an immunologically silent facade (Wyatt & Sodroski, 1998; Wyatt *et al.*, 1998). As a result, mature viral spikes are protected from nAb and other host immune responses by a massive carbohydrate 'glycan shield' (Chen *et al.*, 2005; Wyatt & Sodroski, 1998; Wyatt *et al.*, 1998). In fact, a prominent role of carbohydrates of HIV/SIV in evasion from immune surveillance has been reported previously as follows. Variants of SIV that have evolved to acquire additional glycans in the variable regions of Env have increased neutralization resistance compared with the parental virus (Chackerian *et al.*, 1997; Cheng-Mayer *et al.*, 1999). Similarly, the appearance of neutralization escape mutants has been associated with altered glycosylation in HIV-1 evolved during the course of infection (Wei *et al.*, 2003). Conversely, infection with SIV239 mutants with deglycosylated Env (lacking *N*-linked glycosylation sites) in the variable loops V1/V2 of gp120 elicited markedly increased titres of nAb (Reitter *et al.*, 1998). We have reported that a deglycosylation mutant, Δ5G, lacking *N*-linked glycosylation sites at aa 79, 146, 171, 460 and 479 in gp120 of SIV239 displayed an attenuated phenotype when used to infect rhesus macaques (Mori *et al.*, 2001; Ohgimoto *et al.*, 1998). In addition, animals infected with Δ5G exhibited almost sterile protection against rechallenge with SIV239 (Mori *et al.*, 2001).

Thus, we suggest that studies aimed at identifying the mechanisms underlying the early and potent immune control of deglycosylated SIV may provide knowledge for the formulation of effective HIV/SIV vaccines. Studies performed herein were therefore directed at attempts to define more precisely the early humoral responses (both virus-specific nAb and non-nAb) generated after infection with Δ5G in rhesus macaques and to compare these responses with those observed in macaques inoculated with wild-type SIV239, with the rationale that results from such studies may help to identify their potential contribution towards viral control of primary infection.

METHODS

Viruses. The molecular pathogenic clone of SIV239 (Regier & Desrosiers, 1990) and its derived deglycosylated mutant, Δ5G, were used in this study. Δ5G was derived by mutagenesis of an SIV239 infectious DNA clone so that the asparagine residues for *N*-glycosylation at aa 79, 146, 171, 460 and 479 in gp120 were converted to glutamine residues (Fig. 1a) (Ohgimoto *et al.*, 1998). Viral stocks of SIV239 and Δ5G were prepared as reported previously (Mori *et al.*, 2001).

Peptides. A series of 72 consecutive 25 mer peptides overlapping by 13 aa were synthesized based on the entire SIV239 Env sequence (Env-1–72). These peptides were synthesized by the Microchemical Facility, Emory University School of Medicine, Atlanta, USA. Another set of 15 mer peptides overlapping by 11 aa around the V1/V2 region in gp120 (V1V2-1–12) was synthesized by Sigma-Aldrich Japan based on the Δ5G sequence (see Fig. 5b). All peptides were dissolved in DMSO diluted in PBS.

Animal infection. Juvenile rhesus macaques originating from Myanmar (Burma) (Mm12, Mm13, Mm20, Mm23 and Mm26) or from Laos (Mm07, Mm22 and Mm25) were used following the results of screening for SIV, simian T-cell lymphotropic virus, B virus and type D retrovirus infection, which were all negative prior to inception of the study. All animals were housed in individual cages and maintained according to the rules and guidelines for experimental animal welfare as outlined by the National Institute of Infectious Diseases and National Institute of Biomedical Innovation. Animals were infected intravenously with Δ5G or SIV239 as described previously (Mori *et al.*, 2001).

Plasma viral load measurements. SIV infection was monitored by measuring the plasma viral RNA load using a highly sensitive quantitative real-time RT-PCR. Viral RNA was isolated from plasma samples from infected animals using a commercial viral RNA isolation kit (Roche Diagnostics). SIV *gag* RNA was amplified and quantified using a method originally developed by Hofmann-Lehmann *et al.* (2000) using a TaqMan EZ RT-PCR kit (Applied Biosystems). The detection sensitivity of plasma viral RNA by this method was 100 viral RNA copies per ml plasma (given as copies ml^{-1}).

Neutralization assay. SIV neutralization was tested according to a protocol using CEMx174/SIVLTR-SEAP cells, originally described by Means *et al.* (1997). To measure low levels of nAb, IgG was purified from plasma as described below and concentrated virus stocks were used.

Anti-gp120 Ab ELISA and anti-Env peptide ELISA. Recombinant SIV239 gp120 and Δ5G gp120 were expressed utilizing a Sendai virus vector as described previously (Mori *et al.*, 2005; Yu *et al.*, 1997). Culture supernatant containing approximately 2 μg secreted SIV gp120 ml^{-1} was diluted with an equal amount of PBS, dispensed into each well of an ELISA plate and allowed to incubate at 4 °C overnight.

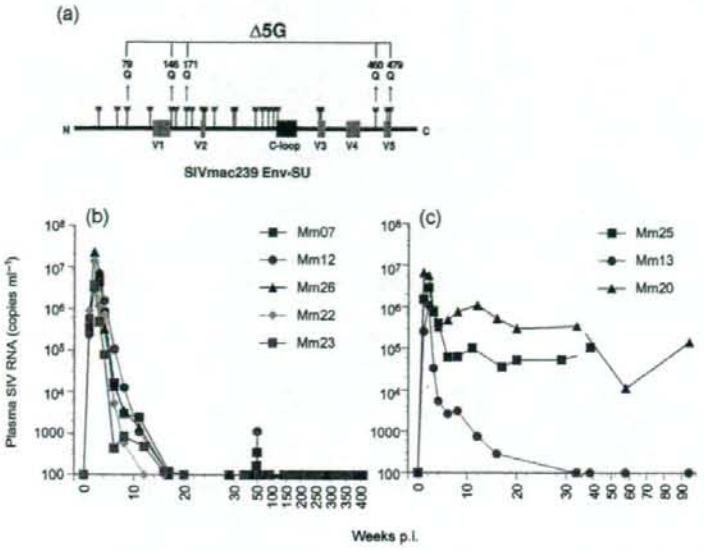

Fig. 1. Plasma SIV RNA loads in animals infected with Δ5G or SIV239. (a) *N*-Glycosylation sites in SIV239 gp120 and deglycosylation sites in Δ5G gp120. The locations of 23 *N*-glycosylation sites in SIV239 gp120, variable regions (V1–V5) and cysteine loops (C-loop) are shown. Δ5G was deglycosylated by N→Q substitutions at aa 79, 146, 171, 460 and 479 in Env (Ohgimoto *et al.*, 1998). (b, c) Plasma viral load in Δ5G-infected (b) and SIV239-infected (c) animals was measured in plasma samples using sensitive real-time RT-PCR to indicate when viral loads declined below 100 copies ml^{-1}. Three Δ5G-infected animals (Mm07, Mm12 and Mm26) were challenged with SIV239 at 48 weeks p.i.; thus, slightly increased viral loads were detected in those animals during weeks 49–51 p.i. (Mori *et al.*, 2001).

For the peptide ELISA, each peptide was diluted to 0.5 μM with 50 mM carbonate buffer (pH 9.5) and captured on Nunc Immobilizer amino plates (Nalge Nunc) at 4 °C overnight. A 1 : 100 dilution (150 μl) of the plasma sample to be tested was dispensed into antigen-immobilized plates and incubated at 37 °C for 1 h. Ab responses were detected using peroxidase-conjugated goat anti-monkey IgG and *o*-phenylenediamine. Absorbance was measured at 490 nm.

Removal of linear V1/V2 epitope-specific Abs from IgG fractions. A mixture of the peptides (V1V2-9, -10 and -11; see Fig. 5b) was conjugated to a HiTrap NHS-activated HP column (GE Healthcare). IgGs from plasma samples were fractionated using a mAb trap kit (GE Healthcare) and applied to the peptide-conjugated column. The flow-through fractions devoid of anti-V1V2-9, -10 and -11 peptide-specific Abs were collected. The concentration of IgG was determined using a protein assay kit (Bio-Rad).

Virion capture assay. The virion capture assay was modified using a method reported by Nyambi *et al.* (1998). ELISA plates were coated with the IgG samples described above at a concentration of 20 μg ml^{-1} in 50 mM carbonate buffer (pH 9.5) and incubated at 4 °C for 48 h. The plates were washed three times with PBS and blocked with 3% BSA in PBS at 37 °C for 1 h. The plates were then washed three times with serum-free RPMI 1640. Δ5G or SIV239 virion solutions with a $p27^{gag}$ concentration of 15, 7.5 and 3.75 ng in 10% fetal bovine serum/RPMI 1640 were added to each well of the IgG-coated plate and incubated at 37 °C for 3 h. The wells were washed five times with serum-free RPMI 1640 to remove unbound virus. The virus bound to IgG was lysed using MagNA Pure LC Lysis/Binding Buffer (Roche Diagnostics). The viral lysates were subjected to viral RNA purification using a MagNA Pure Compact nucleic acid purification kit (Roche Diagnostics). The copy number of the isolated SIV RNA was determined by real-time RT-PCR for SIV239 as described above.

Statistical analysis. Correlation analysis was done using Spearman's non-parametric rank test and the Mann–Whitney test using GraphPad Prism 4.0 software. Correlations were considered to be statistically significant for values of $P<0.05$.

RESULTS

Plasma viral loads of a quintuple deglycosylated SIV239 mutant in rhesus macaques

Eight rhesus macaques were infected intravenously with Δ5G ($n=5$) or SIV239 ($n=3$) (Mori *et al.*, 2001). Plasma viral RNA loads were assayed for up to 400 weeks p.i. and the data obtained in the Δ5G-infected (Fig. 1b) or SIV239-infected (Fig. 1c) animals were plotted. Both Δ5G and SIV239 replicated with similar kinetics during the early phase of primary infection for up to 4 weeks p.i. However, subsequent to this acute infection phase, virus replication was markedly different in the two groups of monkeys: SIV239-infected animals exhibited viral load set points around 10^5 copies ml^{-1} in two of three animals, with one animal (Mm13) having an undetectable viral load (<100 copies ml^{-1}) by 30 weeks p.i. (Fig. 1c). In contrast, the Δ5G-infected animals showed uniformly controlled viraemia reaching undetectable levels by 12–16 weeks p.i. and maintained this control for more than 6 years p.i. (Fig. 1b).

nAb response in Δ5G-infected animals

Although failure to detect a nAb response is characteristic of SIV239-infected rhesus macaques (Johnson *et al.*, 2003; Means *et al.*, 1997), the rapid control of viraemia in Δ5G-infected animals prompted us to determine whether nAb played a role in this control of viraemia. We hypothesized that the deglycosylation might lead to the elicitation of a markedly more vigorous nAb response than infection with SIV239. To maximize the detection sensitivity of weak nAb responses at early time points p.i., an assay that measures neutralization titres based on 50% inhibition of virus replication (IC_{50}) in $CD4^+$ T-cell lines was initially used.